https://doi.org/10.5194/acp-2022-636
Preprint. Discussion started: 13 September 2022


Atmospheric Chemistry and Physics Discussions

# Large differences of highly oxygenated organic molecules (HOMs) and low volatile species in SOA formed from ozonolysis of β-pinene and limonene

Dandan Liu[1#], Yun Zhang[2,3#], Shujun Zhong[1], Shuang Chen[1], Qiaorong Xie[1], Donghuan Zhang[1], Qiang Zhang[1], Wei Hu[1], Junjun Deng[1], Libin Wu[1], Chao Ma[1], Haijie Tong[4,5], Pingqing Fu[1]

[1]Institute of Surface-Earth System Science, School of Earth System Science, Tianjin University, Tianjin 300072, China
[2]Innovation Center of Pesticide Research, Department of Applied Chemistry, College of Science, China Agricultural University, Beijing 100193, China
[3]Institute of Chemistry, Johannes Gutenberg University, Mainz 55128, Germany
[4]Multiphase Chemistry Department, Max Planck Institute for Chemistry, Mainz 55128, Germany
[5]Institute of Surface Science, Helmholtz-Zentrum Hereon, Geesthacht 21502, Germany
# These authors contributed to this study equally.

*Correspondence to:* Haijie Tong (haijie.tong@hereon.de); Pingqing Fu (fupingqing@tju.edu.cn).

**Abstract.** Secondary organic aerosols (SOA) play a key role in climate change and public health. However, the oxidation state and volatility of SOA are still not well understood. Here, we investigated the highly oxygenated organic molecules (HOMs) in SOA formed from ozonolysis of β-pinene and limonene. Fourier transform ion cyclotron resonance mass spectrometry (FT-ICR MS) was used to characterize HOMs, and a scanning mobility particle sizer (SMPS) was used to measure the concentration and size distribution of SOA particles. The abundance of HOMs in limonene SOA was 5-13% higher than in β-pinene SOA (3-13%) exhibiting different trends with increasing ozone concentrations. β-pinene oxidation-derived HOMs prefer to stabilize at high ozone concentration, accompanied by substantial formation of ultra-low-volatility organic compounds (ULVOCs). Limonene-oxidation-derived HOMs prefer to stabilize at moderate ozone concentrations, with semi-, low-, and extremely low-volatility organic compounds (SVOCs, LOVCs, and ELVOCs) play a major role. Combined experimental evidence and theoretical analysis indicate that oxygen-increasing-based peroxy radical chemistry is a plausible mechanism for the formation of compounds with 10 carbon atoms. Our findings show that HOMs and low volatile species in β-pinene and limonene SOA are largely different. The ozone concentration-driven SOA formation and evolution mechanism of monoterpenes is suggested to be considered in future climate or exposure risk models, which may enable more accurate air quality prediction and management.

https://doi.org/10.5194/acp-2022-636
Preprint. Discussion started: 13 September 2022


Atmospheric Chemistry and Physics Discussions

## 1 Introduction

Secondary organic aerosols (SOA) are key component of airborne particulate matter, which play a crucial role in air quality, public health, climate, and hydrological cycle (Laden et al., 2006; Cohen et al., 2017; Kourtchev et al., 2016; Jokinen et al., 2015; Tröstl et al., 2016; Perraud et al., 2012; Ramanathan et al., 2001; Noziere et al., 2015). Monoterpenes ($C_{10}H_{16}$) are a class of biogenic source volatile organic compounds (BVOCs) acting as important precursors of SOA (Kanakidou et al., 2005; Hallquist et al., 2009; Ehn et al., 2012; Fu et al., 2009). SOA formation is a complex multiphase process (Shrivastava et al., 2017), in which biogenic SOA can be formed via the peroxyl radical ($RO_2$) chemistry of BVOCs initiated by ozone ($O_3$), nitrate radicals ($NO_3$), and hydroxyl radicals ($^{\bullet}OH$), etc. (Hallquist et al., 2009; Griffin et al., 1999; Jokinen et al., 2014). These competitive oxidation processes depend on the nature of the parent VOC and atmospheric conditions (Mahilang et al., 2021). However, our current understanding of the mechanisms of SOA formation is limited and the impact of biogenic emissions on global climate remains uncertain (Hallquist et al., 2009; Shah et al., 2019).

SOA contains organic species with a wide range of volatility, which has a strong temperature-dependence (Hallquist et al., 2009; Simon et al., 2020). In contrast, ambient species are thought to consist mainly of low volatile species, potentially reducing the atmospheric relevance of laboratory-generated SOA (Kim and Paulson, 2013). As SOA functionalization and oxygenated compounds increase, the vapor pressure decreases and gaseous compounds condense on existing particles or nucleate to form new compound particles (Donahue et al., 2012; Saukko et al., 2012). Ozonolysis as the most effective formation pathway of semi-, low-, or extremely low-volatile organic compounds (ELVOCs) that contribute significantly to SOA formation (Kroll and Seinfeld, 2008; Kirkby et al., 2016). Recent experimental results have shown that BVOCs can produce large amounts of aerosol particles by forming ultra-low-volatility organic compounds (ULVOCs) even in the absence of sulfuric acid (Kirkby et al., 2016; Guo et al., 2022). In particular, the (extremely) low volatility of the oligomer, it is expected that its irreversible distribution on the aerosol surface will be enhanced (Zhang et al., 2017). Moreover, ELVOCs play a crucial role in the generation of atmospheric cloud condensation nuclei (Kerminen et al., 2012). ELVOCs are mainly derived from monoterpene oxidation and enhance new particle formation in most continental regions (Jokinen et al., 2015). And a key starting point for the formation and growth of new particles is the formation of highly oxidized organic molecules (HOMs), which are a class of organic compounds with a variety of functionalities and a large amount of oxygen atoms (Ehn et al., 2014). HOMs with high oxygen-containing but low oxidation state should determine the oxidation potential of ambient fine particles and laboratory-generated SOA (Tong et al., 2019). HOMs refer to the process of autoxidation in which a $RO_2$ undergoes an intramolecular hydrogen atom shift (H-shift) to form a hydroperoxide functionality (HOO-) and an alkyl radical (RO), and then molecular oxygen rapidly attaches to form a new more oxidized $RO_2$, and this process is repeated several times (Bianchi et al., 2019). Recent research has shown that after a single oxidant attack, the BVOCs can be oxidized to low-volatility aerosol precursors on sub-second timescales, which are then decomposed into aerosols, and even participate in the formation of new particles (Iyer et al., 2021). Laboratory studies of HOMs observed by ozonolysis of monoterpenes are closely corresponded to observations from boreal forests (Ehn et al., 2012; Ehn et al., 2014). Bianchi et al. (2019) have described the relation between

https://doi.org/10.5194/acp-2022-636
Preprint. Discussion started: 13 September 2022


Atmospheric Chemistry and Physics Discussions

HOMs and the volatility classes. The classes are ULVOCs/ELVOCs, low-volatile organic compounds (LVOCs), and semi-volatile organic compounds (SVOCs). Among them, HOMs are an important component of (E)LVOCs, and a small part may be volatile enough to be classified as SVOCs (Li et al., 2019). The ELVOCs in this paper refer to formula for calculating the volatility of organic aerosols based on effective saturation mass concentrations ($3\times10^{-9} < C_0 < 3\times10^{-5}$ μg $m^{-3}$) according to Schervish and Donahue (Schervish and Donahue, 2020), while the HOMs are determined on the basis of the oxygen number in a formula (see section 2.4).

Due to their low volatility, monoterpene HOMs can provide nucleation conditions for the early growth of nanoparticles (Tröstl et al., 2016). The more abundant atmospheric β-pinene and limonene, which are used in this study, are released approximately 30.3 Tg $yr^{-1}$ globally (Guenther et al., 2012). The molecules of β-pinene and limonene have the same number of carbon and hydrogen atoms as well as double bond equivalents (DBE). β-pinene has a bicyclic structure with an exocyclic double bond as the second-most-abundant-VOC and limonene has a monocyclic structure with an exocyclic and an endocyclic double bond, though the endocyclic double bond is more reactive (Gallimore et al., 2017; Kenseth et al., 2018). Thus, even at low concentrations in the atmosphere, limonene has a high potential for SOA formation due to its greater reactivity toward ozone (Tomaz et al., 2021; Bianchi et al., 2019). For limonene, the attack of ozone takes place predominantly on the endocyclic double bond, and for β-pinene, it is the only reactive site. Laboratory studies have shown that the molar yield of HOMs by β-pinene ozonolysis is much lower than that of limonene ozonolysis (Ehn et al., 2014; Jokinen et al., 2015). The ozone chemistry-based SOA formation potential of these two compounds (limonene > β-pinene) is described in other literature (Lee et al., 2006; Jokinen et al., 2015). Notably, β-pinene and limonene showed opposite trends in SOA formation potential under the condition of ·OH oxidation (Jokinen et al., 2015; Mutzel et al., 2016). This reflects that BVOCs in the atmosphere exhibit diverse oxidation chemistry and have different product responses.

The nucleation rate of monoterpene SOA is largely dependent on oxidant types and concentrations. For instance, Zhao et al. found that the SOA yield of ozone degradation of monoterpenes was higher than that of ·OH oxidation (Zhao et al., 2015). Moreover, the initial nucleation of limonene SOA was found to be maximum at low ozone concentrations, while the opposite behavior was observed at high ozone concentrations (Waring et al., 2011). In addition, high BVOC emissions has been found to increase surface ozone and SOA levels in China (Wu et al., 2020). Laboratory studies often use high concentrations of ozone to reduce the loss of semi-volatile vapors to the walls of the chamber (Pathak et al., 2008). To deepen the understanding of ozone concentration-dependent SOA formation mechanisms, it is necessary to study the effect of ozone concentration on the molecular composition of monoterpene SOA particularly the volatility and oxidation state driven constituents (e.g., HOMs and ELVOCs).

The aim of this study was to analyze the influence of ozone concentration on the chemical composition of SOA formed from β-pinene and limonene ozonolysis. The experiments were carried out in a flow tube reactor at three gradient ozone concentrations. Then Fourier transform ion cyclotron resonance mass spectrometer equipped with a 7 Tesla superconducting magnet (7T FT-ICR MS) was used to obtain the molecular composition and reaction mechanism of polar SOA organic extracted with ultrapure Milli-Q water. These efforts provide highly accurate mass measurements of organic compounds to

https://doi.org/10.5194/acp-2022-636
Preprint. Discussion started: 13 September 2022


Atmospheric Chemistry and Physics Discussions

clearly assign molecular formulas including carbon, hydrogen, and oxygen up to 850 Da to explore the difference of particulate HOMs originating from β-pinene and limonene oxidation.

## 2 Method

### 2.1 Laboratory SOA generation and collection

A schematic description of the experimental procedure used in this study is shown in Figure 1. Laboratory SOA were generated by gas-phase ozonolysis of β-pinene or limonene in a 7 L quartz flow tube reactor. More detailed information about this reactor has been described in previous studies (Tong et al., 2016; Tong et al., 2019). Briefly, 1 mL of β-pinene (99%, Sigma Aldrich) or limonene (99%, Sigma Aldrich) were separately kept in 1.5 mL amber glass vials (VWR International GmbH) as SOA precursor sources. Flows of 1 bar and 1 standard liter per minute $N_2$ (99.999%, Westfalen AG) were used as a carrier gas to introduce the evaporated volatile organic compounds (VOC) into the reactor for ~5 min gas-phase ozonolysis reaction. The $O_3$ was generated via passing synthetic air (Westfalen AG, 1.8~2.1 L $min^{-1}$) through a 185 nm UV light ($O_3$ generator, L.O.T.-Oriel GmbH & Co. KG). The ozone concentrations in the flow tube reactor were 50±10 ppb, 315±20 ppb or 565±20 ppb, which were measured with an ozone monitor (model 49i, Thermo Fisher Scientific Inc.). On the basis of a calibration function measured by gas chromatography−mass spectrometry, the precursor concentration was estimated to be in the range of 1~2 ppm for β-pinene and limonene. The reaction conditions are shown in Table S1. Ozonolysis of β-pinene and limonene SOA were performed under dark and dry conditions to reduce the complexity of SOA formation. Seed aerosols and hydroxyl radical scavenger were not added. When concentrations of β-pinene SOA, limonene SOA, and ozone are stable, the SOA were collected twice in a row for each ozone concentration condition on 47 mm diameter Omnipore Teflon filters (JVWP04700, Merck Chemicals GmbH). The sampling time varied from several minutes to several hours depending on the required aerosol mass. SOA filter samples were wrapped in aluminum foil and kept cool during transport between laboratories. A scanning mobility particle sizer (SMPS, GRIMM Aerosol Technik GmbH & Co. KG) was used to characterize the size distribution and number concentration of the generated SOA. A flow rate of ~3 L $min^{-1}$ was controlled using a common diaphragm vacuum pump (0~3 L $min^{-1}$), which was connected after the aerosol samplers. Experimental tests confirmed that blank filters did not produce aqueous phase radicals. The condensation of water vapor on a filter during SOA collection and wall loss were negligible in this study. A Teflon filter with particle loading was weighed using XSE105DU balance with accuracy of ±10 μg.

### 2.2 FT-ICR MS measurement

The β-pinene and limonene SOA filter samples and blank filters were extracted three times with ultrapure Milli-Q water. Each extraction was carried out in a sonicating ice bath for 10 min. The extracts were combined and added to a solid-phase extraction (SPE) cartridge (Oasis HLB, Waters Corporation, 60 mg, 3 mL) on the Supelco Visiprep SPE Vacuum Manifold (USA), which had been preconditioned with 3×6 mL methanol and Milli-Q water, respectively. Then, the cartridges were washed three times

https://doi.org/10.5194/acp-2022-636
Preprint. Discussion started: 13 September 2022


Atmospheric Chemistry and Physics Discussions

with 6 mL Millipore Q water and dried under a nitrogen flow for around 1 h. Subsequently, the organic compounds retained on the cartridge were eluted using 6 mL of methanol. The eluate was immediately concentrated to about 10 µL by a rotary evaporator and sample concentrator to achieve the minimum detection concentration for detection. Low molecular weight compounds (<100 Da) are expected to excluded in the rinsing and drying step of extraction, as reported by Bianco et al (Bianco et al., 2018). Finally, the eluate was stored at -20 °C in a brown glass vial with TEFLON® cap until analysis.

The chemical composition of organics for pretreated extracts were finally analyzed with a 7 T FT-ICR MS (Bruker Daltonik, GmbH, Bremen, Germany) equipped with an electrospray ionization (ESI) ion source at the School of Earth System Science, Tianjin University, Tianjin, China. The instrument was externally calibrated in the negative ion mode with Suwannee River fulvic acid (SRFC) and the resulting mass accuracy was better than 1 ppm. Because the target species were water-soluble polar compounds, all the samples were analyzed in the negative ionization mode and infused into the ESI unit by syringe infusion at a flow rate of 220 µL $h^{-1}$. Ions were accumulated for 0.05 s in the hexapole collision cell. For each mass spectra were from 150 to 1000 Da. The ESI capillary voltage was 5.0 kV and the spectra are the accumulation of 256 scans. An average resolving power (m/Δm 50 %) of over 400 000 (at mass-to-charge (m/z) 400 Da) was achieved. The capillary temperature was maintained at 200 °C. Filter blank was analyzed following the same procedure as the aerosol sample analysis. Other details of the experiment setup can be found elsewhere (Cao et al., 2016; Xie et al., 2020a).

### 2.3 Molecular formula assignment

The original FT-ICR MS data was processed using Data Analysis 5.0 (Bruker Daltonics). The mass spectra were internally recalibrated using an abundant homologous series of oxygen-containing organic compounds in the samples over the mass range between 150 and 1000 Da. Molecular formulae were assigned for peaks with a signal-to-noise (S/N) ratio ≥ 4 by allowing a mass error threshold of ±1 ppm between the measured and theoretically calculated mass. The molecular formula calculator was set to calculate formulae in the mass range between 150 and 800 Da with elemental compositions up to 40 carbon (C), 80 hydrogen (H), and 30 oxygen (O) atoms with a tolerance of ±1 ppm when only C, H and O are studied. Furthermore, DBE must be an integer value, the elemental ratio limits of hydrogen-to-carbon ratio (H/C) (0.3~2.5), oxygen-to-carbon ratio (O/C) (0~1.2) and a nitrogen rule for even electron ions were used to eliminate chemically unreasonable formula (Koch et al., 2005). Unambiguous molecular formula assignment was determined with help of the homologous series approach for improving the reliability on multiple formula assignments (Koch et al., 2007). No isotopic peaks were considered in this study. To minimize the effects of the experimental procedure, all samples were subtracted from the blank test for organic molecules with the S/N ≥ 20 and intensity greater than those of the analyzed samples. The lower peak intensity of common ions suggests they resulted from carry-over within the electrospray ionization source (Kundu et al., 2012). In addition, because of the instrument limitation, the absolute mass concentration of each compound cannot be obtained.

The assigned molecular formulae were examined using the DBE and Kendrick mass defect (KMD) series (Wu et al., 2004). To assess the saturation and oxidation degree of β-pinene and limonene SOA, the value of DBE is calculated along Eq. (1).

$$DBE = 1 + C - 0.5H \quad , \tag{1}$$

https://doi.org/10.5194/acp-2022-636
Preprint. Discussion started: 13 September 2022


Atmospheric Chemistry and Physics Discussions

where *C* and *H* are the number of carbon and hydrogen atoms, respectively.

The maximum carbonyl ratio (MCR) was used to estimate the contribution of carbonyl equivalent groups in the molecule with oxygen number greater than or equal to DBE (Zhang et al., 2021). The value of MCR is calculated as Eq. (2).

$$MCR = \frac{DBE}{O} \quad , \tag{2}$$

where *O* is the number of oxygen atoms in the formula. Based on the MCR values, the HOMs were categorized into 4 groups: (I) very highly oxidized organic compounds (VHOOCs; $0 \leq MCR \leq 0.2$), (II) highly oxidized organic compounds (HOOCs; $0.2 < MCR \leq 0.5$), (III) intermediately oxidized organic compounds (IOOCs; $0.5 < MCR \leq 0.9$), and (IV) oxidized unsaturated organic compounds (OUOCs; $0.9 < MCR \leq 1$).

The carbon oxidation states ($OS_C$) is used to describe the composition of complex mixtures of organic matter undergoing oxidation processes. $OS_C$ is calculated as follows (Kroll et al., 2011):

$$OS_C = 2O/C - H/C \quad , \tag{3}$$

The weighted average of molecular weight (MW), O atom, O/C ratio, $OS_C$ and DBE was calculated using Eq. (4).

$$X = \sum(Int_i \times X_i) / \sum Int_i \quad , \tag{4}$$

where *X* is the weighted average of parameter above, $X_i$ is the parameter values above and $Int_i$ is the relative intensity for each individual formula, $i$.

Molecular corridors can help to constrain chemical and physical properties as well as reaction rates and pathways involved in organic aerosol evolution (Shiraiwa et al., 2014). Saturation vapor pressure ($C_0$) is a consequence of the molecular characteristics of molar mass, chemical composition, and structure. Li et al. have developed a parameterization to estimate $C_0$ as $log_{10}C_0 = f(n_C, n_O)$ (Li et al., 2016). The $C_0$ is defined by the 2D volatility basis set (2D-VBS) as follows,

$$log_{10}C_0 = (n_c^0 - n_C)b_C - n_O b_O - 2\frac{n_C n_O}{n_C - n_O} b_{CO} \quad , \tag{5}$$

where $n_c^0$ is the reference carbon number; $n_C$ and $n_O$ denote the number of carbon and oxygen atoms, respectively; $b_C$ and $b_O$ denote the contribution of each kind of atoms to $log_{10}C_0$, respectively, and $b_{CO}$ is the carbon-oxygen nonideality (Donahue et al., 2011). The above parameters obtained at 298 K of this work were adapted to the work of Li et al. (2016). The target compounds were grouped into (I) intermediate-volatility organic compounds (IVOCs; $300 < C_0 < 3 \times 10^6$ μg m$^{-3}$), (II) semi-volatility organic compounds (SVOCs; $0.3 < C_0 < 300$ μg m$^{-3}$), (III) low-volatility organic compounds (LVOCs; $3 \times 10^{-5} < C_0 < 0.3$ μg m$^{-3}$), (IV) extremely low-volatility organic compounds (ELVOCs; $3 \times 10^{-9} < C_0 < 3 \times 10^{-5}$ μg m$^{-3}$) and (V) ultra-low-volatility organic compounds (ULVOCs; $C_0 < 3 \times 10^{-9}$ μg m$^{-3}$) (Donahue et al., 2011; Bianchi et al., 2019; Schervish and Donahue, 2020).

In order to compare the composition difference between β-pinene SOA and limonene SOA, the data of the samples collected twice for the corresponding conditions were integrated and pooled in a subsequent study to investigate the effect of ozone concentration on the organic fraction.

### 2.4 Determination of highly oxygenated molecules (HOMs)

https://doi.org/10.5194/acp-2022-636
Preprint. Discussion started: 13 September 2022


Atmospheric Chemistry and Physics Discussions

Due to their low saturation vapor pressure, HOMs are low-volatility organic compounds (LVOCs) or even extremely low-volatility organic compounds (ELVOCs) (Vogel et al., 2016). In this study, HOMs with molecular formulae of $C_{8\text{-}10}H_{12\text{-}16}O_{6\text{-}9}$ and $C_{17\text{-}20}H_{26\text{-}32}O_{8\text{-}15}$ were used for assigning the detected monomers and dimers formed from monoterpene ozonolysis, and compounds with O/C ratio < 0.7 was used to filter out non-HOM monomers (Tong et al., 2019; Tröstl et al., 2016; Tu et al., 2016). The formation pathways of HOMs were estimated based on previous research, and mainly through hydroperoxide channel and Criegee channel (Tomaz et al., 2021; Shen et al., 2021; Kundu et al., 2012). In this paper, monomer refers to $C_{8\sim10}$ molecule, dimer refers to $C_{17\sim20}$ molecule.

## 3 Results and discussion

### 3.1 Effects of ozone concentration on size distribution and oxidation state of SOA

Particle size distributions of β-pinene SOA and limonene SOA are shown in Figure 2, which typically ranged from 20 to 200 nm, and the median diameters of the mass size distribution were 35∼80 nm. The ozone concentration elevation increased the particle size and number concentration of β-pinene SOA and limonene SOA, which may be due to the formation of high molecular weight and low-volatile dimers (Kristensen et al., 2014). The low-volatile organics promote the formation and growth of molecular clusters and survive to cloud condensation nuclei-active sizes (Shrivastava et al., 2017). At 50 ppb ozone concentration, the particle size of limonene SOA exhibit a broader distribution than β-pinene SOA, indicating a plausible different partition and agglomeration kinetics of them.

The weighted average of MW, O atom, O/C ratio, DBE and $OS_C$ increased with the increase of ozone concentration (Table 1). It shows that high oxidation and high carbon number organic matter prefer to form at high ozone concentration, and most of the less oxidized organic molecules may be converted into highly oxidized organic molecules (HOMs). Results also show that high ozone concentration tends to increase oxygen reaction. This may indicate the importance of ozone in the formation of particulate organic peroxides by ozonation of β-pinene. The higher abundance of organic peroxides in β-pinene SOA than limonene SOA can explain the higher yield of ˙OH of β-pinene SOA in liquid water (Tong et al., 2016). Figure S1 shows that the total intensity of the organic signal in the β-pinene SOA sample increased significantly with the increase of ozone concentration, while the number of organic molecules reached the maximum value at 315 ppb ozone concentration. In contrast, the total intensity of the organic signal in the limonene SOA sample reached the maximum value at 315 ppb ozone concentration, and the number of organic molecules decreased significantly with the increase of ozone concentration. The peak intensity of MW ranged from 350 to 450 Da, with β-pinene SOA exhibit a maximum proportion at 565 ppb ozone, but limonene SOA have the highest proportion at 315 ppb. This trend indicates that MW of biogenic SOA formed from different precursors have different responses to ozonolysis.

Table S2 shows that for β-pinene SOA, the predominant molecules are m/z = 274 ($C_{17}H_{26}O_4$) and m/z = 183 ($C_{10}H_{16}O_3$, pinonic acid) (Jaoui and Kamens, 2003) at 50 ppb ozone concentration, and m/z = 337 ($C_{19}H_{30}O_5$), m/z = 183 ($C_{10}H_{16}O_3$), m/z = 186

https://doi.org/10.5194/acp-2022-636
Preprint. Discussion started: 13 September 2022


Atmospheric Chemistry and Physics Discussions

($C_9H_{14}O_4$) and m/z = 370 ($C_{19}H_{30}O_7$) at 315 ppb and 565 ppb ozone concentration. A higher abundance of m/z = 474 ($C_{32}H_{42}O_3$) molecule was only found in β-pinene SOA formed at 50 ppb ozone condition, which is high carbon-containing and less oxygen-containing compound, indicating that β-pinene ozonolysis products prefer carbon-carbon bonding or oligomerizing at low ozone concentration. The mostly abundant organics in limonene SOA is always the molecule of m/z = 199 ($C_{10}H_{16}O_4$, 7-hydroxy limononic acid) in three ozone concentrations, which has also been observed as a major product from limonene oxidation by ozone (Kundu et al., 2012; Gallimore et al., 2017; Hammes et al., 2019). At 50 ppb ozone concentration, both β-pinene SOA and limonene SOA exhibited higher abundance of organic molecules with less oxygen-containing (monomer: O ≤ 2 and dimer: O ≤ 4), while the abundance of organic molecules with less oxygen-containing was quite low at 565 ppb ozone condition. This indicates that high ozone concentration is not conducive to the formation of less oxygen-containing organic molecules or promotes the conversion of less oxidized organic molecules into high oxygen-containing organic molecules.

For limonene SOA, when the ozone concentration is increased from 315 ppb to 565 ppb, the MW, O atom and DBE are decreased, indicating that the high carbon-containing and oxygen-containing organic molecules in limonene SOA may crack at high ozone concentration to form low carbon number and less oxidized organic molecules. The element characteristic values of SOA produced by limonene were generally higher than those of β-pinene, probably due to the faster rate at which ozonolysis proceeds for limonene ($k_{limonene+O_3} = 2.1 \times 10^{-16}$ cm$^3$ molecules$^{-1}$ s$^{-1}$) as compared to β-pinene ($k_{\beta\text{-pinene}+O_3} = 1.5 \times 10^{-17}$ cm$^3$ molecules$^{-1}$ s$^{-1}$) (Atkinson and Arey, 2003). This shows that limonene is preferred to proceed oxygenate and accretion reaction than β-pinene. Compared to the precursor β-pinene, the unique SOA formed by ozonation of limonene is more concentrated in high $OS_C$ and O/C ratio, as well as low H/C ratio organic molecules. It seems that the condensation reaction channel of limonene is more important than β-pinene. Perhaps the high oxygen-containing organic matter contributes more to the larger size particles of molecular clusters.

The maximum carbonyl ratio (MCR) index is suggested as a tool for a better characterization of the sources and the processing of atmospheric OA components (Zhang et al., 2021). Figure 3 shows the β-pinene SOA- and limonene SOA-contained HOMs depicted in an MCR-Van Krevelen (VK) diagram. The largest fraction of β-pinene SOA components at 565 ppb ozone concentration (66%) and the largest fraction of limonene SOA components at 315 ppb ozone concentration (59%) are located in region II, while only a few compounds show up in region I and IV. Such a distribution pattern indicates that most HOMs formed from ozone-oxidation of β-pinene and limonene are moderately oxidized with MCR values of 0.2∼0.5 and only a few of them with MCR values between 0∼0.2. The organic compounds with higher relative abundance (RA) fall mainly in the region III. Interestingly, the larger RA value HOMs in β-pinene SOA increased, whereas the larger RA value HOMs in limonene SOA decreased with increasing ozone concentration. It seems that the 565 ppb ozone concentration had some inhibitory effect on the oxidation of limonene to form HOMs.

### 3.2 Composition and relative abundance of HOMs in β-pinene and limonene SOA

https://doi.org/10.5194/acp-2022-636
Preprint. Discussion started: 13 September 2022


Atmospheric Chemistry and Physics Discussions

As shown in Figure 4, the identified HOMs mainly exist as dimers with *m/z* of 350~450 Da. Therein, the limonene SOA has higher $RA_{HOMs}$ than β-pinene SOA. As the ozone concentration increased from 50 to 315 ppb, the peak number-based $RA_{HOMs}$ in β-pinene and limonene SOA kept constant to be ~3% and ~5%, whereas the peak intensity-based $RA_{HOMs}$ increased significantly from 3% to 7% and 14% to 20%, respectively. This indicates that HOMs yield rather than chemical composition diversity of β-pinene and limonene SOA responded to the increasing oxidation degree of precursors. As the ozone concentration is increased further to 565 ppb, both of the peak number- and peak intensity-based $RA_{HOMs}$ in β-pinene SOA increased significantly to 13% and 5%, respectively. In contrast, and the peak number-based $RA_{HOMs}$ in limonene SOA did not change, and the peak intensity-based $RA_{HOMs}$ even decreased slightly to 18%. Thus, we estimate that under high ozone concentration conditions, the ozonolysis of β-pinene produced more HOMs, whereas the overoxidation and disassociation of preformed particulate HOMs may happen to limonene SOA.

Figure 5 shows the O/C, H/C, carbon number and $OS_C$ of common or unique molecules in β-pinene SOA, limonene SOA, or HOMs formed under three ozone concentrations. The comparison revealed that the number of molecules formed by ozonation of β-pinene was higher than by limonene. The distribution of oxidation states in the unique molecules of β-pinene SOA was broad and mostly in the region of lower O/C ratio, while the unique molecules in limonene SOA were distributed in higher $OS_C$ and lower H/C ratio (Figure 5a and 5b), indicating a higher ozonation degree of limonene than that of β-pinene. The HOMs in Figure 5c and 5d showed a similar variation trend as the SOA, confirming the contribution of HOMs to the formation of biogenic SOA.

The identified HOMs in β-pinene and limonene SOA are categorized into groups with different carbon number ($C_n$) or oligomer clusters and their RA are plotted versus the ozone concentration in Figure 6. Figure 6a shows that the respective distribution pattern of HOM monomers in β-pinene and limonene SOA kept the same under different ozone concentrations. Therein, the HOM monomers in limonene SOA are mostly exist as $C_{10}$ species, while HOM monomers in β-pinene SOA mainly comprise compounds with eight carbon atoms ($C_8$). This may be due to the fact that the carbon backbone of endocyclic limonene is retained on ozonolysis, whereas the terminal vinylic carbon of exocyclic β-pinene is cleaved (Ma and Marston, 2008; Kundu et al., 2012). Figure 6b shows that the $RA_{HOMs}$ dimmers in β-pinene and limonene SOA exhibits different variation trends as the increasing of ozone concentrations. About the β-pinene SOA, the carbon numbers of HOM dimmers have the same pattern at 50 and 315 ppb ozone concentrations, with the RA increased from $C_{17}$ to $C_{18}$ and then gradually decreased for $C_{19}$ and $C_{20}$ species. However, at 565 ppb ozone condition, the RA of HOM dimers continually decreased from $C_{17}$ to $C_{20}$ compounds. In contrast, the $C_n$ pattern of HOM dimers in limonene SOA kept the same under different ozone concentrations, which reached a maximum for $C_{19}$ species. The different $C_n$ patterns of HOM dimers in β-pinene and limonene SOA may be due to the front ones tend to form via the combination of $C_8$ and $C_9$ or $C_9$ and $C_9$, whereas the later ones are preferred to form via the combination of $C_{10}$ and $C_9$. Such an inference may also explain the higher averaged carbon number, oxygen number, and molecule weight of limonene SOA than β-pinene SOA (Table 1).

https://doi.org/10.5194/acp-2022-636
Preprint. Discussion started: 13 September 2022


Atmospheric Chemistry and Physics Discussions

### 3.3 Volatility of HOMs in β-pinene and limonene SOA

To explore the volatility of HOMs, the identified HOMs haven been assigned to semi-, low-, and extremely low-volatile organic compounds (SVOCs, LVOCs, and ELVOCs) and their RA were shown in Figure 7. Figure 7a shows that the LVOCs subgroup dominants the peak intensity of both β-pinene and limonene SOA-contained HOMs, the pattern of which resembles the combined RA of SVOCs, LVOCs, and ELVOCs. Moreover, the RA of LVOC type HOMs in β-pinene SOA increases with increasing ozone concentration, while that in limonene SOA reaches the maximum value at the ozone concentration of 315 ppb. Figure 7b shows that formula number-based total RA of SVOCs, LVOCs, and ELVOCs increased as the increasing of ozone concentrations for both β-pinene and limonene SOA, with the RA of LVOCs equivalent to the ELVOCs. Thus, Figure 7 reflects that mass variation of β-pinene and limonene SOA during ozone chemistry are largely driven by LVOCs and ELOVCs. In addition, the peak intensity- and formula number-based $RA_{HOMs}$ of LVOCs and ELVOCs in limonene SOA is significantly higher than that of β-pinene SOA, indicating that LVOCs and ELVOCs contribute more to the HOMs of limonene SOA. These findings agree with previous discovery of limonene ozonolysis to be more efficient than β-pinene ozonolysis in generating ELVOCs (Jokinen et al., 2015). Moreover, the volatility and carbon oxidation state averages of HOMs were also found to change in similar trends as that of LOVCs, ELVOCs, and ULVOCs in SOA, but the trends of β–pinene SOA and limonene SOA are different as shown in Figure S2.

Figure 8 shows the O/C ratio of β-pinene and limonene SOA constituents versus their estimated volatility. Figure 8a-8c shows that the O/C ratio distribution of ULVOCs in β-pinene SOA is broadened as the increase of ozone concentration. Meanwhile, both of O/C ratios and RA of IVOCs, SVOCs, LVOCs, and ELVOCs increased prominently, and the abundance of compounds with low O/C ratios decreased. This indicates that deeper oxidation of β-pinene may decrease the overall volatility of SOA particles via changing the relative abundance of organic matter with different volatilities. Figure 8d-8f shows that O/C ratio and volatility distribution of limonene SOA components vary slightly. This may correlate with the preference of forming highly oxygenated, low-volatility reaction products by limonene via an autoxidation mechanism (Jokinen et al., 2015). Moreover, the enrichment of high RA ELVOCs in limonene SOA confirms that limonene is more likely to form particulate ELVOCs even ULVOCs than β-pinene via ozonolysis, which may be related to the higher reactivity of limonene due to its intrinsic two double bonds and endocyclic structure.

The molecular corridor is a two-dimensional framework of volatility and molecular weight of SOA components bounded by two boundary lines of n-alkanes ($C_nH_{2n+2}$) with O/C = 0 and sugar alcohols ($C_nH_{2n+2}O_n$) with O/C = 1, which helps to explain the physicochemical properties in the evolution of SOA (Li et al., 2016; Xie et al., 2020b). Figure 9 shows the correlation between the volatility and molecular weight of the common and unique molecules of β-pinene SOA and limonene SOA under three ozone conditions. The number of unique organic molecules formed by monoterpene oxidation is higher at 50 ppb ozone concentration, accounting for about 15~20% of the total number of molecules. Furthermore, unique organic molecules at 50 ppb ozone concentration are mainly concentrated in the SVOCs and LVOCs regions, while unique organic molecules at 315 ppb and 565 ppb ozone concentration are mainly concentrated in the ELVOCs and ULVOCs region. Compared to limonene

https://doi.org/10.5194/acp-2022-636
Preprint. Discussion started: 13 September 2022


Atmospheric Chemistry and Physics Discussions

SOA, many low volatile organic components close to the sugar alcohol ($C_nH_{2n+2}O_n$) line were found in β-pinene SOA, indicating that ozone concentration has a greater impact on the SOA formed from ozonolysis of β-pinene. ULVOCs with molar mass of 500~800 g $mol^{-1}$ account for a substantial fraction of β-pinene SOA formed at 565 ppb ozone, whereas the SVOCs, LVOCs, and ELVOCs with molar mass of 200-600 g $mol^{-1}$ dominate the limonene SOA. The volatility difference of β-pinene and limonene SOA associates with the plausible different partition or stabilization mechanisms of HOMs and low volatility species under different ozone concentrations, including the SOA aging related volatilization.

### 3.4 Potential formation mechanisms of HOM monomers and dimers in β-pinene and limonene SOA

Previous study shows that gas-phase monomer and dimer products formed through $RO_2 + RO_2$, $RO_2 + HO_2$, $RO_2$ isomerization, and stabilized Criegee intermediate + carboxylic acid contributed to SOA formation. But aldehydes and ketones are often converted to carboxyl and ester groups by Baeyer-Villiger reactions with the hydroperoxides and peroxyacid in particle phase, while hydroperoxides and peroxyacid are converted to acids, alcohols, or ketones (Claflin et al., 2018). Due to the high activity of these pathways, the dimers with very low volatility are expected to be distributed directly onto particles after gas phase production. The dimers are strongly influenced by particle phase chemistry, possibly involving the combined effects of accretion reactions ($C_{8\text{-}10} + C_{8\text{-}10} \rightarrow C_{17\text{-}20}$) and decomposition of high molecular weight compounds ($C_{20} \rightarrow C_{17\text{-}19}$) (Pospisilova et al., 2020). The formation of HOMs dimers is mainly through the accretion reaction of various HOMs monomers $RO_2$ and the termination reaction of dimer $RO_2$ formed by the further reaction of the closed shell dimer with $O_3$, and they may also be through $C_{10}$ reaction of $RO_2$ with monoterpenes. The HOMs trimers may be formed via the accretion reaction of dimer $RO_2$ and monomer $RO_2$, which will not be analyzed in detail later.

HOMs monomers may be formed via hydroperoxide channel and oxygen-increasing reactions (OIR) of Criegee channel (Tomaz et al., 2021; Shen et al., 2021; Kundu et al., 2012). The possible formation mechanisms of $C_{10}$ HOMs monomers from the β-pinene and limonene ozonolysis are shown in Figure 10. There is a high probability that ozone first reacts with endocyclic double bond of limonene, opens the chain to form Criegee radical, and then formed $C_{10}H_{14}O_7$ and $C_{10}H_{16}O_8$. Ozone concentration had a great influence on HOMs of $C_9$ and $C_{10}$ in β-pinene system, and the formation path is as depicted in Figure S3. Here, a number of series of HOM monomers with $CH_2$ were found (Fig. 11). Among them, $C_{10}H_{16}O_7$ was formed in all three ozone concentrations, but $C_9H_{14}O_7$ and $C_{10}H_{14}O_7$ were formed at 315 ppb and 565 ppb ozone concentrations, and $C_9H_{12}O_7$ was formed at high ozone concentrations. This suggests that β-pinene increases the possibility of carbonyl formation at high ozone concentrations. The formation of $C_{10}H_{16}O_9$ corresponds to the monoterpene oxidation product (Ehn et al., 2014; Berndt et al., 2016; Brean et al., 2019). In this experiment, only β-pinene SOA was detected at high ozone concentration, and the O number of HOMs dimers under this condition could be up to 15, while $C_{10}H_{16}O_9$ was not detected in the limonene SOA, and the maximum O number of the HOMs dimers was 13. This may be due to the fact that the oxidation degree of $RO_2$ termination reaction of some HOMs in β-pinene SOA is higher than that of limonene.

https://doi.org/10.5194/acp-2022-636
Preprint. Discussion started: 13 September 2022


Atmospheric Chemistry and Physics Discussions

The presence of $C_{17}H_{26}O_8$ through the decomposition of $C_{19}H_{28}O_{11}$ with loss of a ketene from the internal containing a labile trioxide functionality, and the conversion of the unstable acyl hydroperoxide groups to carboxyl groups (Kahnt et al., 2018). Tomaz et al. (2021) found that the reaction between $C_{10}H_{15}O_6$ and $C_{10}H_{15}O_8$ radicals may also contribute to the formation of $C_{20}H_{30}O_{12}$ dimer, corresponding monomers and dimers were found in the limonene system, β-pinene at high ozone concentration, $C_{10}H_{16}O_8$ organic matter, and subsequently detected the $C_{20}H_{30}O_{12}$ dimer, which verified this conclusion. The chemical formulas along with suggested molecular structures of the identified dimer compounds are shown in Tables S3. Most of the HOMs products of the two monoterpenes were very similar, while the RA of the different HOMs varied widely, suggesting that the reaction pathways are similar, but the degree of branching in the reaction mechanism is different.

Accretion reactions transform the mass from monomers to oligomers, yielding products with a higher number of carbon atoms and converting semi-volatile molecules into higher-molecular weight compounds with lower saturation vapor concentrations (Barsanti et al., 2017). These reactions have been studied under laboratory conditions and suggested to play an important role in ambient environment (Berndt et al., 2018). This observation shows that the particle-phase chemistry causes changes in the overall SOA composition over the ozone concentration observed here. High molecular weight and low volatile dimer compounds have been identified as important components of environmental compounds. The monomeric building blocks of the dimer esters formed by β-pinene ozonolysis are attributed to one of the dicarboxylic acids, such as $C_9H_{14}O_4$ (*cis*-pinic acid), $C_8H_{12}O_4$ (*cis*-norpinic acid), and $C_8H_{14}O_5$ (diaterpenylic acid), which can be well characterization of pinene oxidation products during dimer formation (Kenseth et al., 2018). Trimer-like compounds are typically in the range of 450∼650 Da (Kundu et al., 2012), with limonene SOA having a higher RA than β-pinene SOA as shown in Figure 4. The formation of trimers is associated with the presence of two double bonds in limonene. One of the C=C double bonds is first oxidized to the dimer products, while the double bond of the other provides a reaction point for further oxidation of the dimers, making it easier to form dimer $RO_2$ radicals (Guo et al., 2022). It is noticeable that the mechanism of dimer formation in similar monoterpene systems remains unresolved and warranty follow up studies (Kenseth et al., 2018).

## 4 Conclusions

The composition of aerosols varies systematically with gas-particle partitioning. At lower mass concentrations, polar components seem to dominate the aerosol, while at higher concentrations, VOCs may condense (Grieshop et al., 2007). Environmental SOA components are considered to be concentration-dependent, in agreement with the results of this paper. HOMs in SOA formed by ozone oxidation are also affected differently by ozone concentration. The precursors of β-pinene and limonene have the same molecular formula but different structures, with β-pinene was found to be more obviously affected. The $RA_{HOMs}$ in β-pinene SOA was more significantly affected by ozone concentration, while that of limonene SOA was almost hardly affected by ozone concentration, which was related to the high activity of limonene with two double bonds and endocyclic structure. β-pinene was found more inclined to form the monomer ($C_8$) and dimer ($C_{17}$) of HOMs, while limonene

https://doi.org/10.5194/acp-2022-636
Preprint. Discussion started: 13 September 2022


Atmospheric Chemistry and Physics Discussions

was more inclined to form HOMs monomer ($C_{10}$) and dimer ($C_{19}$), which is obviously related to the way of broken bonds after ozone oxidation. In addition, distinct volatilities and abundances of HOMs in β-pinene and limonene SOA reflects the different molecular response of particulate reaction products to biogenic precursor oxidation states, leading to different SOA size and number concentration distribution profiles. Higher ozone concentrations (315 ppb and 565 ppb) were favorable for the formation of HOMs and ELVOCs, and the number of unique organic molecules was higher. Compared with β-pinene SOA, the abundance of ELVOCs in limonene SOA contributes more.

In addition to the effect of ozone concentration on HOMs, other oxidants in the atmosphere have different effects on them. For example, $NO_2$ inhibited the formation of highly oxidized dimer products by suppression of autoxidation (Rissanen, 2018).When considerable ·OH was present, the potential dimer sources were also suppressed (Zhang et al., 2017). Moreover, Simon et al. (2020) found a continuous decrease in the oxidation level of α-pinene SOA and yields of HOMs as the temperature decreased from 25 to -50 °C. Similar result was also confirmed in urban field samples (Brean et al., 2020). Current mass spectrometry techniques can only obtain information on the molecular formula of the HOMs, hindering the study of the detailed formation mechanism of many atmospheric precursors. Therefore, experimental conditions and new analytical techniques need to be developed to characterize HOMs rapidly and in detail.

*Data availability*. The dataset for this paper is available upon request from the corresponding author (fupingqing@tju.edu.cn).

*Author contribution.* DL participated in the investigation, methodology, software development, formal analysis, and writing of the original draft. SZ and SC participated in the methodology and formal analysis. YZ collected the samples. All co-authors participated in validation as well as in reviewing and editing of the manuscript. PF and HT participated in the conceptualization, project administration, and funding acquisition.

*Competing interests.* The authors declare that they have no conflict of interests.

*Acknowledgments.* This work was supported by the National Natural Science Foundation of China (NSFC) (Grant Nos. 42130513 and 41625014), Tianjin Research Innovation Project for Postgraduate Students (Grant No. 2021YJSB135), Max Planck Institute for Chemistry, and Helmholtz-Zentrum Hereon. The authors thank Ulrich Pöschl for stimulating discussions.

## References

Atkinson, R. and Arey, J.: Atmospheric degradation of volatile organic compounds, Chem. Rev., 103, 4605-4638, https://doi.org/10.1021/cr0206420, 2003.

Barsanti, K. C., Kroll, J. H., and Thornton, J. A.: Formation of low-volatility organic compounds in the atmosphere: Recent advancements and insights, J. Phys. Chem. Lett., 8, 1503-1511, https://doi.org/10.1021/acs.jpclett.6b02969, 2017.

Berndt, T., Mentler, B., Scholz, W., Fischer, L., Herrmann, H., Kulmala, M., and Hansel, A.: Accretion product formation from ozonolysis and OH radical reaction of α-Pinene: Mechanistic insight and the influence of isoprene and ethylene, Environ. Sci. Technol., 52, 11069-11077, https://doi.org/10.1021/acs.est.8b02210, 2018.

Berndt, T., Richters, S., Jokinen, T., Hyttinen, N., Kurtén, T., Otkjær, R. V., Kjaergaard, H. G., Stratmann, F., Herrmann, H., Sipilä, M., Kulmala, M., and Ehn, M.: Hydroxyl radical-induced formation of highly oxidized organic compounds, Nat. Commun., 7, 13677, https://doi.org/10.1038/ncomms13677, 2016.

Bianchi, F., Kurten, T., Riva, M., Mohr, C., Rissanen, M. P., Roldin, P., Berndt, T., Crounse, J. D., Wennberg, P. O., Mentel, T. F., Wildt, J.,

https://doi.org/10.5194/acp-2022-636
Preprint. Discussion started: 13 September 2022


Atmospheric Chemistry and Physics Discussions

Junninen, H., Jokinen, T., Kulmala, M., Worsnop, D. R., Thornton, J. A., Donahue, N., Kjaergaard, H. G., and Ehn, M.: Highly oxygenated organic molecules (HOM) from gas-phase autoxidation involving peroxy radicals: A key contributor to atmospheric aerosol, Chem. Rev., 119, 3472-3509, https://doi.org/10.1021/acs.chemrev.8b00395, 2019.

Bianco, A., Deguillaume, L., Vaitilingom, M., Nicol, E., Baray, J. L., Chaumerliac, N., and Bridoux, M.: Molecular characterization of cloud water samples collected at the Puy de Dome (France) by Fourier transform ion cyclotron resonance mass spectrometry, Environ. Sci. Technol., 52, 10275-10285, https://doi.org/10.1021/acs.est.8b01964, 2018.

Brean, J., Harrison, R. M., Shi, Z., Beddows, D. C. S., Acton, W. J. F., Hewitt, C. N., Squires, F. A., and Lee, J.: Observations of highly oxidized molecules and particle nucleation in the atmosphere of Beijing, Atmos. Chem. Phys., 19, 14933-14947, https://doi.org/10.5194/acp-19-14933-2019, 2019.

Brean, J., Beddows, D. C. S., Shi, Z., Temime-Roussel, B., Marchand, N., Querol, X., Alastuey, A., Minguillón, M. C., and Harrison, R. M.: Molecular insights into new particle formation in Barcelona, Spain, Atmos. Chem. Phys., 20, 10029-10045, https://doi.org/10.5194/acp-20-10029-2020, 2020.

Cao, D., Lv, J., Geng, F., Rao, Z., Niu, H., Shi, Y., Cai, Y., and Kang, Y.: Ion accumulation time dependent molecular characterization of natural organic matter using electrospray ionization-Fourier transform ion cyclotron resonance mass Spectrometry, Anal. Chem., 88, 12210-12218, https://doi.org/10.1021/acs.analchem.6b03198, 2016.

Claflin, M. S., Krechmer, J. E., Hu, W., Jimenez, J. L., and Ziemann, P. J.: Functional group composition of secondary organic aerosol formed from ozonolysis of α-pinene under high VOC and autoxidation conditions, ACS Earth Space Chem., 2, 1196-1210, https://doi.org/10.1021/acsearthspacechem.8b00117, 2018.

Cohen, A. J., Brauer, M., Burnett, R., Anderson, H. R., Frostad, J., Estep, K., Balakrishnan, K., Brunekreef, B., Dandona, L., Dandona, R., Feigin, V., Freedman, G., Hubbell, B., Jobling, A., Kan, H., Knibbs, L., Liu, Y., Martin, R., Morawska, L., Pope, C. A., Shin, H., Straif, K., Shaddick, G., Thomas, M., van Dingenen, R., van Donkelaar, A., Vos, T., Murray, C. J. L., and Forouzanfar, M. H.: Estimates and 25-year trends of the global burden of disease attributable to ambient air pollution: an analysis of data from the Global Burden of Diseases Study 2015, The Lancet, 389, 1907-1918, https://doi.org/10.1016/S0140-6736(17)30505-6, 2017.

Donahue, N. M., Epstein, S. A., Pandis, S. N., and Robinson, A. L.: A two-dimensional volatility basis set: 1. organic-aerosol mixing thermodynamics, Atmos. Chem. Phys., 11, 3303-3318, https://doi.org/10.5194/acp-11-3303-2011, 2011.

Donahue, N. M., Kroll, J. H., Pandis, S. N., and Robinson, A. L.: A two-dimensional volatility basis set – Part 2: Diagnostics of organic-aerosol evolution, Atmos. Chem. Phys., 12, 615-634, https://doi.org/10.5194/acp-12-615-2012, 2012.

Ehn, M., Kleist, E., Junninen, H., Petäjä, T., Lönn, G., Schobesberger, S., Dal Maso, M., Trimborn, A., Kulmala, M., Worsnop, D. R., Wahner, A., Wildt, J., and Mentel, T. F.: Gas phase formation of extremely oxidized pinene reaction products in chamber and ambient air, Atmos. Chem. Phys., 12, 5113-5127, https://doi.org/10.5194/acp-12-5113-2012, 2012.

Ehn, M., Thornton, J. A., Kleist, E., Sipilä, M., Junninen, H., Pullinen, I., Springer, M., Rubach, F., Tillmann, R., Lee, B., Lopez-Hilfiker, F., Andres, S., Acir, I.-H., Rissanen, M., Jokinen, T., Schobesberger, S., Kangasluoma, J., Kontkanen, J., Nieminen, T., Kurtén, T., Nielsen, L. B., Jørgensen, S., Kjaergaard, H. G., Canagaratna, M., Maso, M. D., Berndt, T., Petäjä, T., Wahner, A., Kerminen, V.-M., Kulmala, M., Worsnop, D. R., Wildt, J., and Mentel, T. F.: A large source of low-volatility secondary organic aerosol, Nature, 506, 476-479, https://doi.org/10.1038/nature13032, 2014.

Fu, P., Kawamura, K., Chen, J., and Barrie, L. A.: Isoprene, monoterpene, and sesquiterpene oxidation products in the high Arctic aerosols during late winter to early summer, Environ. Sci. Technol., 43, 4022-4028, https://doi.org/10.1021/es803669a, 2009.

Gallimore, P. J., Mahon, B. M., Wragg, F. P. H., Fuller, S. J., Giorio, C., Kourtchev, I., and Kalberer, M.: Multiphase composition changes and reactive oxygen species formation during limonene oxidation in the new Cambridge Atmospheric Simulation Chamber (CASC), Atmos. Chem. Phys., 17, 9853-9868, https://doi.org/10.5194/acp-17-9853-2017, 2017.

Grieshop, A. P., Donahue, N. M., and Robinson, A. L.: Is the gas-particle partitioning in alpha-pinene secondary organic aerosol reversible?, Geophys. Res. Lett., 34, L14810, https://doi.org/10.1029/2007gl029987, 2007.

Griffin, R. J., Cocker, D. R., Flagan, R. C., and Seinfeld, J. H.: Organic aerosol formation from the oxidation of biogenic hydrocarbons, J. Geophys. Res.-Atmos., 104, 3555-3567, https://doi.org/10.1029/1998jd100049, 1999.

Guenther, A. B., Jiang, X., Heald, C. L., Sakulyanontvittaya, T., Duhl, T., Emmons, L. K., and Wang, X.: The model of emissions of Gases and Aerosols from Nature version 2.1 (MEGAN2.1): An extended and updated framework for modeling biogenic emissions, Geosci. Model Dev., 5, 1471-1492, https://doi.org/10.5194/gmd-5-1471-2012, 2012.

Guo, Y., Shen, H., Pullinen, I., Luo, H., Kang, S., Vereecken, L., Fuchs, H., Hallquist, M., Acir, I.-H., Tillmann, R., Rohrer, F., Wildt, J., Kiendler-Scharr, A., Wahner, A., Zhao, D., and Mentel, T. F.: Identification of highly oxygenated organic molecules and their role in aerosol formation in the reaction of limonene with nitrate radical, Atmos. Chem. Phys., 22, 11323-11346, https://doi.org/10.5194/acp-22-11323-2022, 2022.

Hallquist, M., Wenger, J. C., Baltensperger, U., Rudich, Y., Simpson, D., Claeys, M., Dommen, J., Donahue, N. M., George, C., Goldstein, A. H., Hamilton, J. F., Herrmann, H., Hoffmann, T., Iinuma, Y., Jang, M., Jenkin, M. E., Jimenez, J. L., Kiendler-Scharr, A., Maenhaut, W., McFiggans, G., Mentel, T. F., Monod, A., Prévôt, A. S. H., Seinfeld, J. H., Surratt, J. D., Szmigielski, R., and Wildt, J.: The formation, properties and impact of secondary organic aerosol: current and emerging issues, Atmos. Chem. Phys., 9, 5155-5236, https://doi.org/10.5194/acp-9-5155-2009, 2009.



Hammes, J., Lutz, A., Mentel, T., Faxon, C., and Hallquist, M.: Carboxylic acids from limonene oxidation by ozone and hydroxyl radicals: insights into mechanisms derived using a FIGAERO-CIMS, Atmos. Chem. Phys., 19, 13037-13052, https://doi.org/10.5194/acp-19-13037-2019, 2019.

Iyer, S., Rissanen, M. P., Valiev, R., Barua, S., Krechmer, J. E., Thornton, J., Ehn, M., and Kurten, T.: Molecular mechanism for rapid autoxidation in α-pinene ozonolysis, Nat. Commun., 12, 878, https://doi.org/10.1038/s41467-021-21172-w, 2021.

Jaoui, M. and Kamens, R. M.: Gaseous and particulate oxidation products analysis of a mixture of α-pinene + β-pinene/$O_3$/air in the absence of light and α-pinene + β-pinene/$NO_x$/air in the presence of natural sunlight, J. Atmos. Chem., 44, 259-297, https://doi.org/10.1023/A:1022977427523, 2003.

Jokinen, T., Sipilä, M., Richters, S., Kerminen, V.-M., Paasonen, P., Stratmann, F., Worsnop, D., Kulmala, M., Ehn, M., Herrmann, H., and Berndt, T.: Rapid autoxidation forms highly oxidized $RO_2$ radicals in the atmosphere, Angew. Chem. Int. Ed. Engl. , 53, 14596-14600, https://doi.org/10.1002/anie.201408566, 2014.

Jokinen, T., Berndt, T., Makkonen, R., Kerminen, V.-M., Junninen, H., Paasonen, P., Stratmann, F., Herrmann, H., Guenther, A. B., Worsnop, D. R., Kulmala, M., Ehn, M., and Sipilä, M.: Production of extremely low volatile organic compounds from biogenic emissions: Measured yields and atmospheric implications, P. Natl. Acad. Sci., 112, 7123-7128, https://doi.org/10.1073/pnas.1423977112, 2015.

Kahnt, A., Vermeylen, R., Iinuma, Y., Safi Shalamzari, M., Maenhaut, W., and Claeys, M.: High-molecular-weight esters in α-pinene ozonolysis secondary organic aerosol: structural characterization and mechanistic proposal for their formation from highly oxygenated molecules, Atmos. Chem. Phys., 18, 8453-8467, https://doi.org/10.5194/acp-18-8453-2018, 2018.

Kanakidou, M., Seinfeld, J. H., Pandis, S. N., Barnes, I., Dentener, F. J., Facchini, M. C., Van Dingenen, R., Ervens, B., Nenes, A., Nielsen, C. J., Swietlicki, E., Putaud, J. P., Balkanski, Y., Fuzzi, S., Horth, J., Moortgat, G. K., Winterhalter, R., Myhre, C. E. L., Tsigaridis, K., Vignati, E., Stephanou, E. G., and Wilson, J.: Organic aerosol and global climate modelling: a review, Atmos. Chem. Phys., 5, 1053-1123, https://doi.org/10.5194/acp-5-1053-2005, 2005.

Kenseth, C. M., Huang, Y., Zhao, R., Dalleska, N. F., Hethcox, J. C., Stoltz, B. M., and Seinfeld, J. H.: Synergistic $O_3$ + OH oxidation pathway to extremely low-volatility dimers revealed in β-pinene secondary organic aerosol, P. Natl. Acad. Sci., 115, 8301-8306, https://doi.org/10.1073/pnas.1804671115, 2018.

Kerminen, V. M., Paramonov, M., Anttila, T., Riipinen, I., Fountoukis, C., Korhonen, H., Asmi, E., Laakso, L., Lihavainen, H., Swietlicki, E., Svenningsson, B., Asmi, A., Pandis, S. N., Kulmala, M., and Petäjä, T.: Cloud condensation nuclei production associated with atmospheric nucleation: a synthesis based on existing literature and new results, Atmos. Chem. Phys., 12, 12037-12059, https://doi.org/10.5194/acp-12-12037-2012, 2012.

Kim, H. and Paulson, S. E.: Real refractive indices and volatility of secondary organic aerosol generated from photooxidation and ozonolysis of limonene, α-pinene and toluene, Atmos. Chem. Phys., 13, 7711-7723, https://doi.org/10.5194/acp-13-7711-2013, 2013.

Kirkby, J., Duplissy, J., Sengupta, K., Frege, C., Gordon, H., Williamson, C., Heinritzi, M., Simon, M., Yan, C., Almeida, J., Tröstl, J., Nieminen, T., Ortega, I. K., Wagner, R., Adamov, A., Amorim, A., Bernhammer, A.-K., Bianchi, F., Breitenlechner, M., Brilke, S., Chen, X., Craven, J., Dias, A., Ehrhart, S., Flagan, R. C., Franchin, A., Fuchs, C., Guida, R., Hakala, J., Hoyle, C. R., Jokinen, T., Junninen, H., Kangasluoma, J., Kim, J., Krapf, M., Kürten, A., Laaksonen, A., Lehtipalo, K., Makhmutov, V., Mathot, S., Molteni, U., Onnela, A., Peräkylä, O., Piel, F., Petäjä, T., Praplan, A. P., Pringle, K., Rap, A., Richards, N. A. D., Riipinen, I., Rissanen, M. P., Rondo, L., Sarnela, N., Schobesberger, S., Scott, C. E., Seinfeld, J. H., Sipilä, M., Steiner, G., Stozhkov, Y., Stratmann, F., Tomé, A., Virtanen, A., Vogel, A. L., Wagner, A. C., Wagner, P. E., Weingartner, E., Wimmer, D., Winkler, P. M., Ye, P., Zhang, X., Hansel, A., Dommen, J., Donahue, N. M., Worsnop, D. R., Baltensperger, U., Kulmala, M., Carslaw, K. S., and Curtius, J.: Ion-induced nucleation of pure biogenic particles, Nature, 533, 521-526, https://doi.org/10.1038/nature17953, 2016.

Koch, B. P., Dittmar, T., Witt, M., and Kattner, G.: Fundamentals of molecular formula assignment to ultrahigh resolution mass data of natural organic matter, Anal. Chem., 79, 1758-1763, https://doi.org/10.1021/ac061949s, 2007.

Koch, B. P., Witt, M., Engbrodt, R., Dittmar, T., and Kattner, G.: Molecular formulae of marine and terrigenous dissolved organic matter detected by electrospray ionization Fourier transform ion cyclotron resonance mass spectrometry, Geochim. Cosmochim. Ac., 69, 3299-3308, https://doi.org/10.1016/j.gca.2005.02.027, 2005.

Kourtchev, I., Giorio, C., Manninen, A., Wilson, E., Mahon, B., Aalto, J., Kajos, M., Venables, D., Ruuskanen, T., Levula, J., Loponen, M., Connors, S., Harris, N., Zhao, D., Kiendler-Scharr, A., Mentel, T., Rudich, Y., Hallquist, M., Doussin, J.-F., Maenhaut, W., Bäck, J., Petäjä, T., Wenger, J., Kulmala, M., and Kalberer, M.: Enhanced Volatile Organic Compounds emissions and organic aerosol mass increase the oligomer content of atmospheric aerosols, Sci. Rep., 6, 35038, https://doi.org/10.1038/srep35038, 2016.

Kristensen, K., Cui, T., Zhang, H., Gold, A., Glasius, M., and Surratt, J. D.: Dimers in α-pinene secondary organic aerosol: Effect of hydroxyl radical, ozone, relative humidity and aerosol acidity, Atmos. Chem. Phys., 14, 4201-4218, https://doi.org/10.5194/acp-14-4201-2014, 2014.

Kroll, J. H. and Seinfeld, J. H.: Chemistry of secondary organic aerosol: Formation and evolution of low-volatility organics in the atmosphere, Atmos. Environ., 42, 3593-3624, https://doi.org/10.1016/j.atmosenv.2008.01.003, 2008.

Kroll, J. H., Donahue, N. M., Jimenez, J. L., Kessler, S. H., Canagaratna, M. R., Wilson, K. R., Altieri, K. E., Mazzoleni, L. R., Wozniak, A. S., Bluhm, H., Mysak, E. R., Smith, J. D., Kolb, C. E., and Worsnop, D. R.: Carbon oxidation state as a metric for describing the chemistry of atmospheric organic aerosol, Nat. Chem., 3, 133-139, https://doi.org/10.1038/nchem.948, 2011.

Kundu, S., Fisseha, R., Putman, A. L., Rahn, T. A., and Mazzoleni, L. R.: High molecular weight SOA formation during limonene ozonolysis:

https://doi.org/10.5194/acp-2022-636
Preprint. Discussion started: 13 September 2022


Atmospheric Chemistry and Physics Discussions

insights from ultrahigh-resolution FT-ICR mass spectrometry characterization, Atmos. Chem. Phys., 12, 5523-5536, https://doi.org/10.5194/acp-12-5523-2012, 2012.
Laden, F., Schwartz, J., Speizer, F. E., and Dockery, D. W.: Reduction in fine particulate air pollution and mortality, Am. J. Resp. Crit. Care, 173, 667-672, https://doi.org/10.1164/rccm.200503-443OC, 2006.
Lee, A., Goldstein, A. H., Kroll, J. H., Ng, N. L., Varutbangkul, V., Flagan, R. C., and Seinfeld, J. H.: Gas-phase products and secondary aerosol yields from the photooxidation of 16 different terpenes, J. Geophys. Res., 111, D17305, https://doi.org/10.1029/2006jd007050, 2006.
Li, X., Chee, S., Hao, J., Abbatt, J. P. D., Jiang, J., and Smith, J. N.: Relative humidity effect on the formation of highly oxidized molecules and new particles during monoterpene oxidation, Atmos. Chem. Phys., 19, 1555-1570, https://doi.org/10.5194/acp-19-1555-2019, 2019.
Li, Y., Pöschl, U., and Shiraiwa, M.: Molecular corridors and parameterizations of volatility in the chemical evolution of organic aerosols, Atmos. Chem. Phys., 16, 3327-3344, https://doi.org/10.5194/acp-16-3327-2016, 2016.
Ma, Y. and Marston, G.: Multifunctional acid formation from the gas-phase ozonolysis of β-pinene, Phys. Chem. Chem. Phys., 10, 6115-6126, https://doi.org/10.1039/b807863g, 2008.
Mahilang, M., Deb, M. K., and Pervez, S.: Biogenic secondary organic aerosols: A review on formation mechanism, analytical challenges and environmental impacts, Chemosphere, 262, 127771, https://doi.org/10.1016/j.chemosphere.2020.127771, 2021.
Mutzel, A., Rodigast, M., Iinuma, Y., Böge, O., and Herrmann, H.: Monoterpene SOA – Contribution of first-generation oxidation products to formation and chemical composition, Atmos. Environ., 130, 136-144, https://doi.org/10.1016/j.atmosenv.2015.10.080, 2016.
Noziere, B., Kalberer, M., Claeys, M., Allan, J., D'Anna, B., Decesari, S., Finessi, E., Glasius, M., Grgic, I., Hamilton, J. F., Hoffmann, T., Iinuma, Y., Jaoui, M., Kahnt, A., Kampf, C. J., Kourtchev, I., Maenhaut, W., Marsden, N., Saarikoski, S., Schnelle-Kreis, J., Surratt, J. D., Szidat, S., Szmigielski, R., and Wisthaler, A.: The molecular identification of organic compounds in the atmosphere: state of the art and challenges, Chem. Rev., 115, 3919-3983, https://doi.org/10.1021/cr5003485, 2015.
Pathak, R., Donahue, N. M., and Pandis, S. N.: Ozonolysis of β-Pinene: Temperature dependence of secondary organic aerosol mass fraction, Environ. Sci. Technol., 42, 5081-5086, https://doi.org/10.1021/es070721z, 2008.
Perraud, V., Bruns, E. A., Ezell, M. J., Johnson, S. N., Yu, Y., Alexander, M. L., Zelenyuk, A., Imre, D., Chang, W. L., Dabdub, D., Pankow, J. F., and Finlayson-Pitts, B. J.: Nonequilibrium atmospheric secondary organic aerosol formation and growth, P. Natl. Acad. Sci., 109, 2836-2841, https://doi.org/10.1073/pnas.1119909109, 2012.
Pospisilova, V., Lopez-Hilfiker, F. D., Bell, D. M., Haddad, I. E., Mohr, C., Huang, W., Heikkinen, L., Xiao, M., Dommen, J., Prevot, A. S. H., Baltensperger, U., and Slowik, J. G.: On the fate of oxygenated organic molecules in atmospheric aerosol particles, Sci. Adv., 6, eaax8922, https://doi.org/10.1126/sciadv.aax8922, 2020.
Ramanathan, V., Crutzen, P. J., Kiehl, J. T., and Rosenfeld, D.: Aerosols, climate, and the hydrological cycle, Science, 294, 2119-2124, https://doi.org/10.1126/science.1064034, 2001.
Rissanen, M. P.: $NO_2$ suppression of autoxidation–inhibition of gas-phase highly oxidized dimer product formation, ACS Earth Space Chem., 2, 1211-1219, https://doi.org/10.1021/acsearthspacechem.8b00123, 2018.
Saukko, E., Lambe, A. T., Massoli, P., Koop, T., Wright, J. P., Croasdale, D. R., Pedernera, D. A., Onasch, T. B., Laaksonen, A., Davidovits, P., Worsnop, D. R., and Virtanen, A.: Humidity-dependent phase state of SOA particles from biogenic and anthropogenic precursors, Atmos. Chem. Phys., 12, 7517-7529, https://doi.org/10.5194/acp-12-7517-2012, 2012.
Schervish, M. and Donahue, N. M.: Peroxy radical chemistry and the volatility basis set, Atmos. Chem. Phys., 20, 1183-1199, https://doi.org/10.5194/acp-20-1183-2020, 2020.
Shah, R. U., Coggon, M. M., Gkatzelis, G. I., McDonald, B. C., Tasoglou, A., Huber, H., Gilman, J., Warneke, C., Robinson, A. L., and Presto, A. A.: Urban oxidation flow reactor measurements reveal significant secondary organic aerosol contributions from volatile emissions of emerging importance, Environ. Sci. Technol., 54, 714-725, https://doi.org/10.1021/acs.est.9b06531, 2019.
Shen, H., Zhao, D., Pullinen, I., Kang, S., Vereecken, L., Fuchs, H., Acir, I. H., Tillmann, R., Rohrer, F., Wildt, J., Kiendler-Scharr, A., Wahner, A., and Mentel, T. F.: Highly oxygenated organic nitrates formed from $NO_3$ radical-initiated oxidation of β-pinene, Environ. Sci. Technol., 55, 15658-15671, https://doi.org/10.1021/acs.est.1c03978, 2021.
Shiraiwa, M., Berkemeier, T., Schilling-Fahnestock, K. A., Seinfeld, J. H., and Pöschl, U.: Molecular corridors and kinetic regimes in the multiphase chemical evolution of secondary organic aerosol, Atmos. Chem. Phys., 14, 8323-8341, https://doi.org/10.5194/acp-14-8323-2014, 2014.
Shrivastava, M., Cappa, C. D., Fan, J., Goldstein, A. H., Guenther, A. B., Jimenez, J. L., Kuang, C., Laskin, A., Martin, S. T., Ng, N. L., Petaja, T., Pierce, J. R., Rasch, P. J., Roldin, P., Seinfeld, J. H., Shilling, J., Smith, J. N., Thornton, J. A., Volkamer, R., Wang, J., Worsnop, D. R., Zaveri, R. A., Zelenyuk, A., and Zhang, Q.: Recent advances in understanding secondary organic aerosol: Implications for global climate forcing, Rev. Geophys., 55, 509-559, https://doi.org/10.1002/2016rg000540, 2017.
Simon, M., Dada, L., Heinritzi, M., Scholz, W., Stolzenburg, D., Fischer, L., Wagner, A. C., Kürten, A., Rörup, B., He, X.-C., Almeida, J., Baalbaki, R., Baccarini, A., Bauer, P. S., Beck, L., Bergen, A., Bianchi, F., Bräkling, S., Brilke, S., Caudillo, L., Chen, D., Chu, B., Dias, A., Draper, D. C., Duplissy, J., El-Haddad, I., Finkenzeller, H., Frege, C., Gonzalez-Carracedo, L., Gordon, H., Granzin, M., Hakala, J., Hofbauer, V., Hoyle, C. R., Kim, C., Kong, W., Lamkaddam, H., Lee, C. P., Lehtipalo, K., Leiminger, M., Mai, H., Manninen, H. E., Marie, G., Marten, R., Mentler, B., Molteni, U., Nichman, L., Nie, W., Ojdanic, A., Onnela, A., Partoll, E., Petäjä, T., Pfeifer, J., Philippov, M., Quéléver, L. L. J., Ranjithkumar, A., Rissanen, M. P., Schallhart, S., Schobesberger, S., Schuchmann, S., Shen, J., Sipilä, M., Steiner, G., Stozhkov, Y.,



Tauber, C., Tham, Y. J., Tomé, A. R., Vazquez-Pufleau, M., Vogel, A. L., Wagner, R., Wang, M., Wang, D. S., Wang, Y., Weber, S. K., Wu, Y., Xiao, M., Yan, C., Ye, P., Ye, Q., Zauner-Wieczorek, M., Zhou, X., Baltensperger, U., Dommen, J., Flagan, R. C., Hansel, A., Kulmala, M., Volkamer, R., Winkler, P. M., Worsnop, D. R., Donahue, N. M., Kirkby, J., and Curtius, J.: Molecular understanding of new-particle formation from α-pinene between −50 and +25 °C, Atmos. Chem. Phys., 20, 9183-9207, https://doi.org/10.5194/acp-20-9183-2020, 2020.

Tomaz, S., Wang, D., Zabalegui, N., Li, D., Lamkaddam, H., Bachmeier, F., Vogel, A., Monge, M. E., Perrier, S., Baltensperger, U., George, C., Rissanen, M., Ehn, M., El Haddad, I., and Riva, M.: Structures and reactivity of peroxy radicals and dimeric products revealed by online tandem mass spectrometry, Nat. Commun., 12, 300, https://doi.org/10.1038/s41467-020-20532-2, 2021.

Tong, H., Arangio, A. M., Lakey, P. S. J., Berkemeier, T., Liu, F., Kampf, C. J., Brune, W. H., Pöschl, U., and Shiraiwa, M.: Hydroxyl radicals from secondary organic aerosol decomposition in water, Atmos. Chem. Phys., 16, 1761-1771, https://doi.org/10.5194/acp-16-1761-2016, 2016.

Tong, H., Zhang, Y., Filippi, A., Wang, T., Li, C., Liu, F., Leppla, D., Kourtchev, I., Wang, K., Keskinen, H.-M., Levula, J. T., Arangio, A. M., Shen, F., Ditas, F., Martin, S. T., Artaxo, P., Godoi, R. H. M., Yamamoto, C. I., de Souza, R. A. F., Huang, R.-J., Berkemeier, T., Wang, Y., Su, H., Cheng, Y., Pope, F. D., Fu, P., Yao, M., Pöhlker, C., Petäjä, T., Kulmala, M., Andreae, M. O., Shiraiwa, M., Pöschl, U., Hoffmann, T., and Kalberer, M.: Radical formation by fine particulate matter associated with highly oxygenated molecules, Environ. Sci. Technol., 53, 12506-12518, https://doi.org/10.1021/acs.est.9b05149, 2019.

Tröstl, J., Chuang, W. K., Gordon, H., Heinritzi, M., Yan, C., Molteni, U., Ahlm, L., Frege, C., Bianchi, F., Wagner, R., Simon, M., Lehtipalo, K., Williamson, C., Craven, J. S., Duplissy, J., Adamov, A., Almeida, J., Bernhammer, A.-K., Breitenlechner, M., Brilke, S., Dias, A., Ehrhart, S., Flagan, R. C., Franchin, A., Fuchs, C., Guida, R., Gysel, M., Hansel, A., Hoyle, C. R., Jokinen, T., Junninen, H., Kangasluoma, J., Keskinen, H., Kim, J., Krapf, M., Kürten, A., Laaksonen, A., Lawler, M., Leiminger, M., Mathot, S., Möhler, O., Nieminen, T., Onnela, A., Petäjä, T., Piel, F. M., Miettinen, P., Rissanen, M. P., Rondo, L., Sarnela, N., Schobesberger, S., Sengupta, K., Sipilä, M., Smith, J. N., Steiner, G., Tomè, A., Virtanen, A., Wagner, A. C., Weingartner, E., Wimmer, D., Winkler, P. M., Ye, P., Carslaw, K. S., Curtius, J., Dommen, J., Kirkby, J., Kulmala, M., Riipinen, I., Worsnop, D. R., Donahue, N. M., and Baltensperger, U.: The role of low-volatility organic compounds in initial particle growth in the atmosphere, Nature, 533, 527-531, https://doi.org/10.1038/nature18271, 2016.

Tu, P., Hall, W. A., and Johnston, M. V.: Characterization of highly oxidized molecules in fresh and aged biogenic secondary organic aerosol, Anal. Chem., 88, 4495-4501, https://doi.org/10.1021/acs.analchem.6b00378, 2016.

Vogel, A. L., Schneider, J., Müller-Tautges, C., Klimach, T., and Hoffmann, T.: Aerosol chemistry resolved by mass spectrometry: Insights into particle growth after ambient new particle formation, Environ. Sci. Technol., 50, 10814-10822, https://doi.org/10.1021/acs.est.6b01673, 2016.

Waring, M. S., Wells, J. R., and Siegel, J. A.: Secondary organic aerosol formation from ozone reactions with single terpenoids and terpenoid mixtures, Atmos. Environ., 45, 4235-4242, https://doi.org/10.1016/j.atmosenv.2011.05.001, 2011.

Wu, K., Yang, X., Chen, D., Gu, S., Lu, Y., Jiang, Q., Wang, K., Ou, Y., Qian, Y., Shao, P., and Lu, S.: Estimation of biogenic VOC emissions and their corresponding impact on ozone and secondary organic aerosol formation in China, Atmos. Res., 231, 104656, https://doi.org/10.1016/j.atmosres.2019.104656, 2020.

Wu, Z., Rodgers, R. P., and Marshall, A. G.: Two- and three-dimensional van Krevelen diagrams: A graphical analysis complementary to the kendrick mass plot for sorting elemental compositions of complex organic mixtures based on ultrahigh-resolution broadband Fourier transform ion cyclotron resonance mass measurements, Anal. Chem., 76, 2511-2516, https://doi.org/10.1021/ac0355449, 2004.

Xie, Q., Su, S., Chen, S., Xu, Y., Cao, D., Chen, J., Ren, L., Yue, S., Zhao, W., Sun, Y., Wang, Z., Tong, H., Su, H., Cheng, Y., Kawamura, K., Jiang, G., Liu, C.-Q., and Fu, P.: Molecular characterization of firework-related urban aerosols using Fourier transform ion cyclotron resonance mass spectrometry, Atmos. Chem. Phys., 20, 6803-6820, https://doi.org/10.5194/acp-20-6803-2020, 2020a.

Xie, Q., Li, Y., Yue, S., Su, S., Cao, D., Xu, Y., Chen, J., Tong, H., Su, H., Cheng, Y., Zhao, W., Hu, W., Wang, Z., Yang, T., Pan, X., Sun, Y., Wang, Z., Liu, C. Q., Kawamura, K., Jiang, G., Shiraiwa, M., and Fu, P.: Increase of high molecular weight organosulfate with intensifying urban air pollution in the megacity Beijing, J. Geophys. Res.-Atmos., 125, e2019JD032200, https://doi.org/10.1029/2019jd032200, 2020b.

Zhang, X., Lambe, A. T., Upshur, M. A., Brooks, W. A., Gray Bé, A., Thomson, R. J., Geiger, F. M., Surratt, J. D., Zhang, Z., Gold, A., Graf, S., Cubison, M. J., Groessl, M., Jayne, J. T., Worsnop, D. R., and Canagaratna, M. R.: Highly oxygenated multifunctional compounds in α-pinene secondary organic aerosol, Environ. Sci. Technol., 51, 5932-5940, https://doi.org/10.1021/acs.est.6b06588, 2017.

Zhang, Y., Wang, K., Tong, H., Huang, R. J., and Hoffmann, T.: The maximum carbonyl ratio (MCR) as a new index for the structural classification of secondary organic aerosol components, Rapid Commun. Mass Sp., 35, e9113, https://doi.org/10.1002/rcm.9113, 2021.

Zhao, D. F., Kaminski, M., Schlag, P., Fuchs, H., Acir, I. H., Bohn, B., Häseler, R., Kiendler-Scharr, A., Rohrer, F., Tillmann, R., Wang, M. J., Wegener, R., Wildt, J., Wahner, A., and Mentel, T. F.: Secondary organic aerosol formation from hydroxyl radical oxidation and ozonolysis of monoterpenes, Atmos. Chem. Phys., 15, 991-1012, https://doi.org/10.5194/acp-15-991-2015, 2015.

https://doi.org/10.5194/acp-2022-636
Preprint. Discussion started: 13 September 2022


Atmospheric Chemistry and Physics Discussions

**Table 1.** The chemical characteristics of β-pinene and limonene SOA samples.

| $[O_3]$ / ppbs | MW | O | O/C | DBE | $OS_C$ | Volatility fractions (%) | | | | |
|---|---|---|---|---|---|---|---|---|---|---|
| | | | | | | ULVOCs | ELVOCs | LVOCs | SVOCs | IVOCs |
| β-Pinene SOA | | | | | | | | | | |
| 50 | 305 | 4.77 | 0.30 | 4.69 | -0.98 | 14 | 28 | 33 | 17 | 8 |
| 315 | 307 | 5.49 | 0.35 | 4.40 | -0.89 | 24 | 23 | 28 | 17 | 8 |
| 565 | 319 | 5.93 | 0.37 | 4.54 | -0.84 | 30 | 23 | 23 | 16 | 8 |
| Limonene SOA | | | | | | | | | | |
| 50 | 326 | 6.07 | 0.36 | 4.78 | -0.82 | 12 | 21 | 30 | 25 | 12 |
| 315 | 349 | 6.88 | 0.39 | 4.99 | -0.76 | 26 | 21 | 22 | 21 | 10 |
| 565 | 339 | 6.58 | 0.38 | 4.87 | -0.78 | 26 | 21 | 23 | 20 | 10 |

635

https://doi.org/10.5194/acp-2022-636
Preprint. Discussion started: 13 September 2022


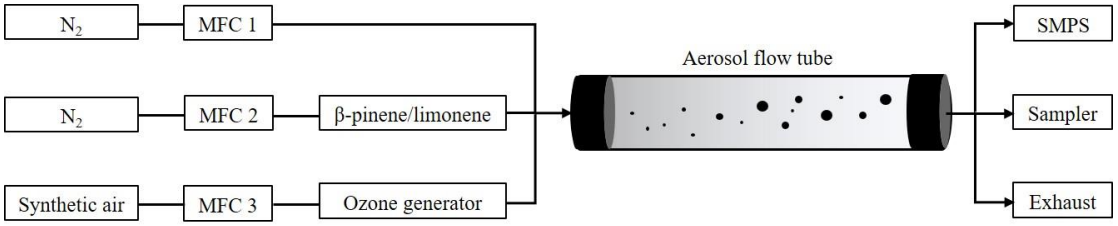


**Figure 1.** Schematic of the experimental setup for generation and collection of SOA. MFC: mass flow controller. SMPS: scanning mobility particle sizer.

https://doi.org/10.5194/acp-2022-636
Preprint. Discussion started: 13 September 2022


Atmospheric Chemistry and Physics Discussions

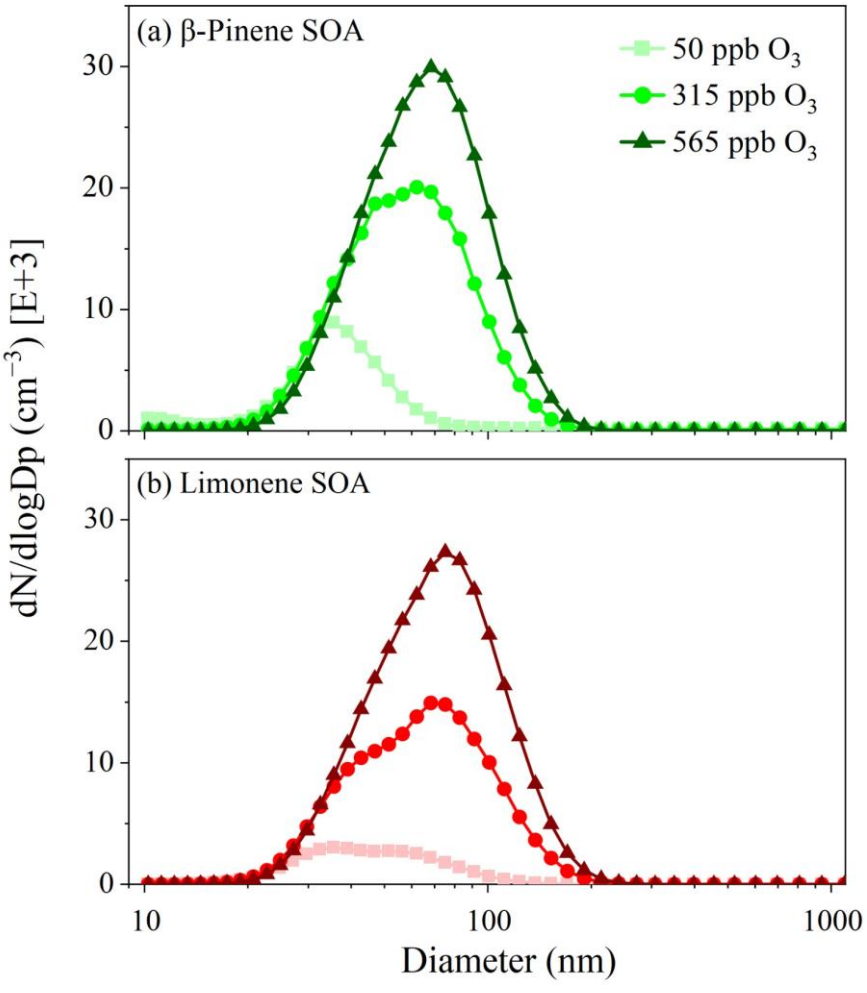


640

**Figure 2.** Distribution of the apparent particle sizes as measured by SMPS of β-pinene SOA (a) and limonene SOA (b).

https://doi.org/10.5194/acp-2022-636
Preprint. Discussion started: 13 September 2022


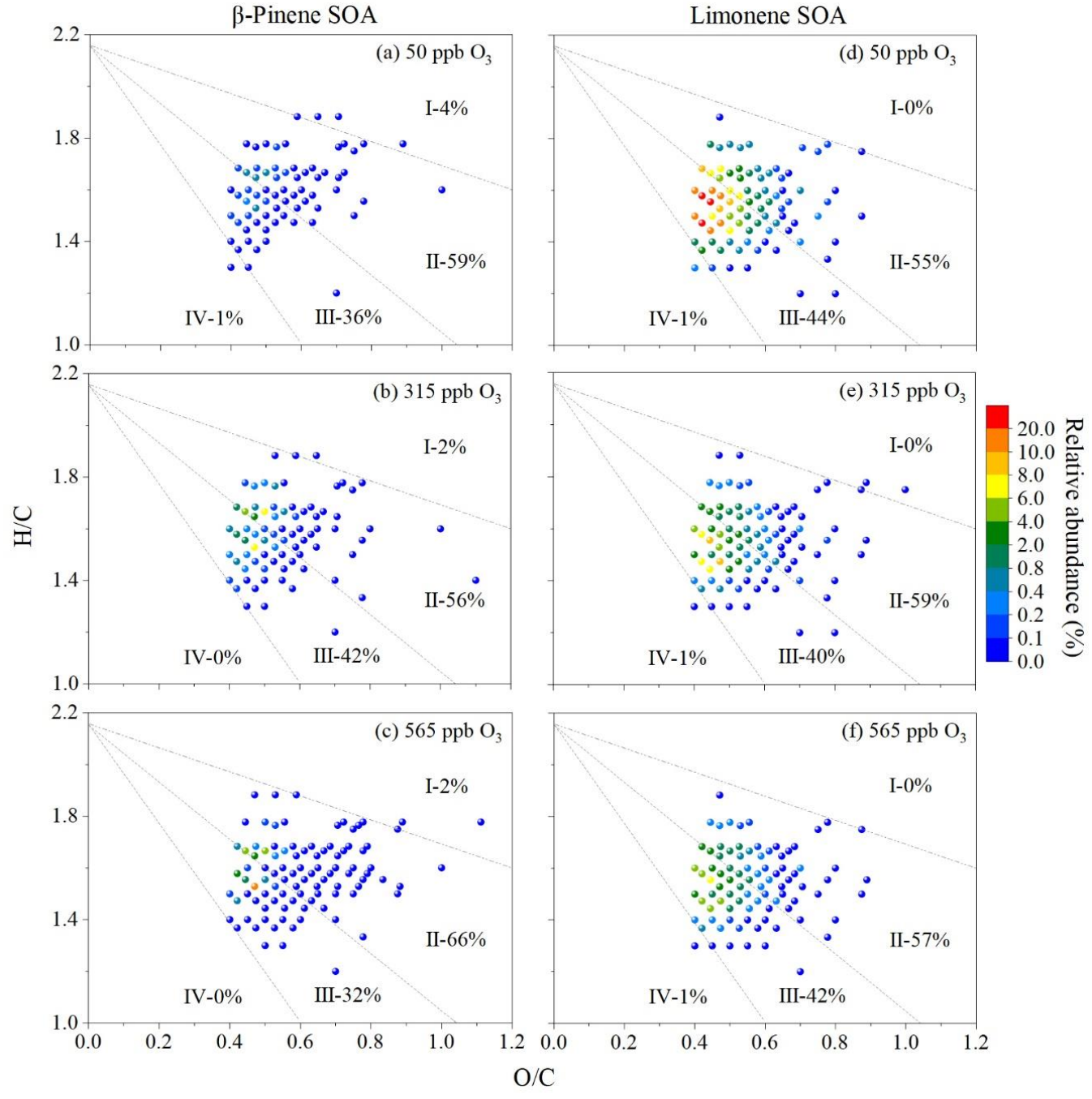


**Figure 3.** MCR-VK diagrams of β-pinene SOA (a, b, c) and limonene SOA (d, e, f) that formed at different ozone concentrations. The colors of the dots indicate the relative abundances of compounds.

https://doi.org/10.5194/acp-2022-636
Preprint. Discussion started: 13 September 2022


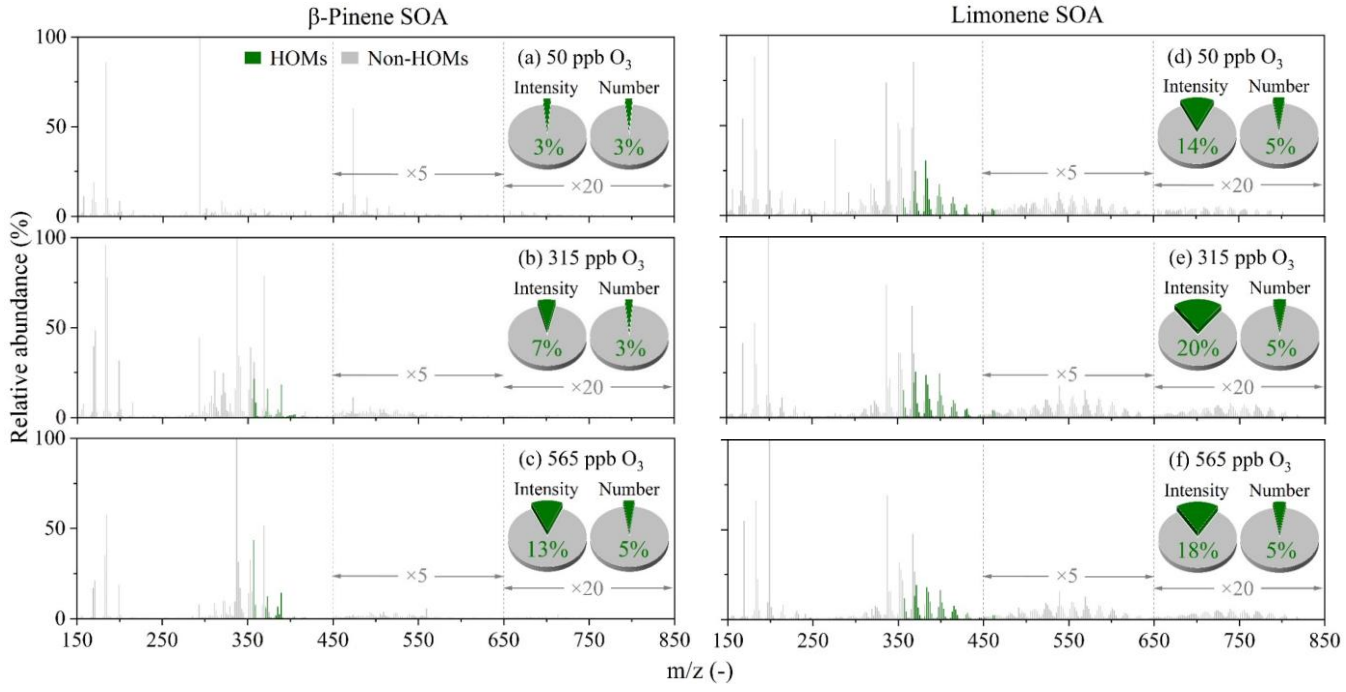


**Figure 4.** Mass spectral fingerprint and relative abundances of HOMs (green) and non-HOMs (gray) in β-pinene SOA (a, b, c) and limonene SOA (d, e, f) that formed at different concentrations of ozone. The relative abundances of compounds with m/z 450 - 650 and 650 - 850 were increased by factors of 5 and 20, respectively. The pie charts indicate the ion intensity- and ion number- based relative abundances of different compounds.

https://doi.org/10.5194/acp-2022-636
Preprint. Discussion started: 13 September 2022


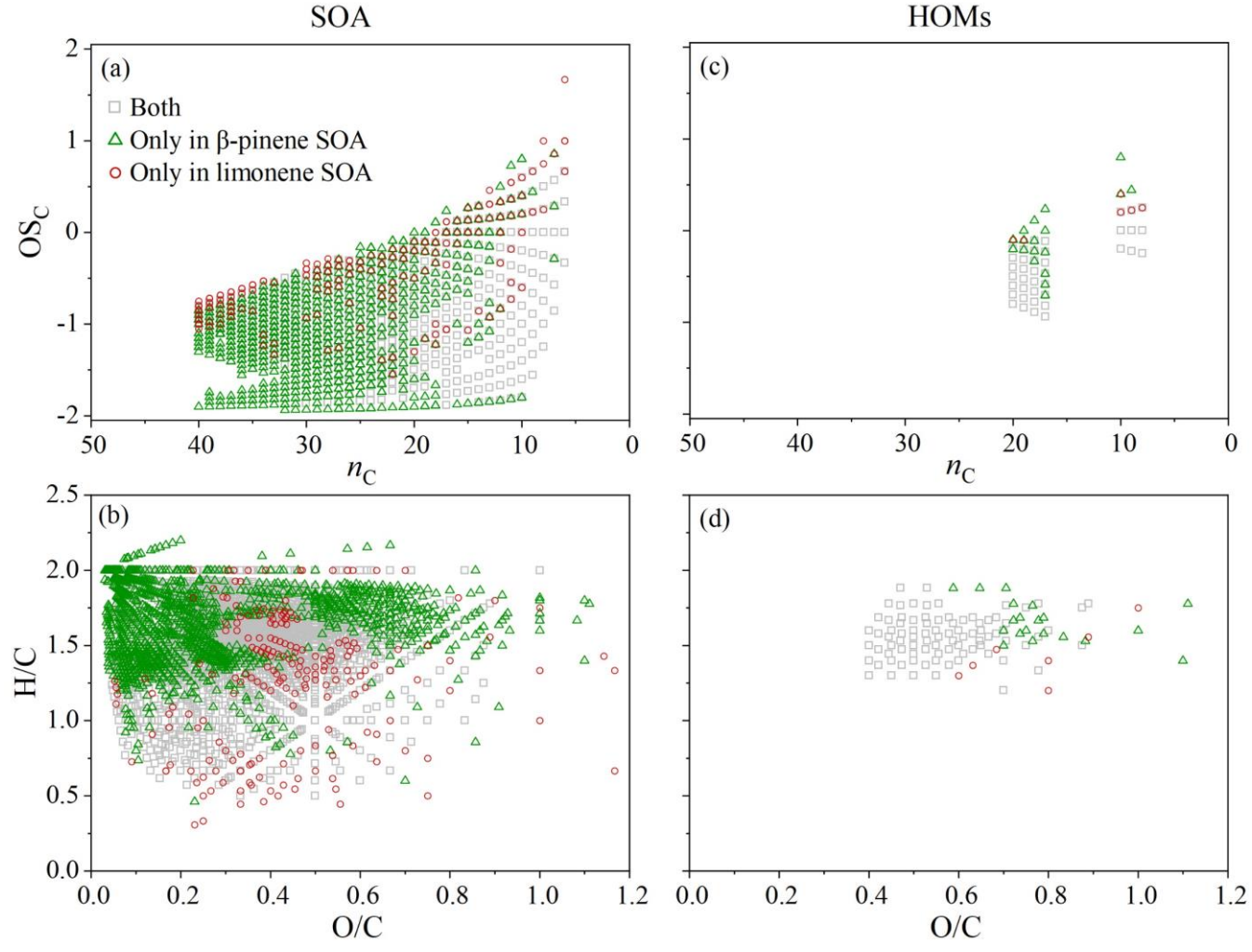


**Figure 5.** The carbon oxidation state ($OS_C$) vs. the number of C atoms ($n_C$) (a, c) and Van Krevelen diagrams (b, d) for the unique assigned formulas from β-pinene SOA and limonene SOA and the corresponding HOMs (c, d). Gray squares represent assigned formulas observed both in β-pinene SOA and limonene SOA. Green triangles and red circles represent assigned formulas observed only in β-pinene SOA and limonene SOA, respectively.

https://doi.org/10.5194/acp-2022-636
Preprint. Discussion started: 13 September 2022




Atmospheric Chemistry and Physics Discussions

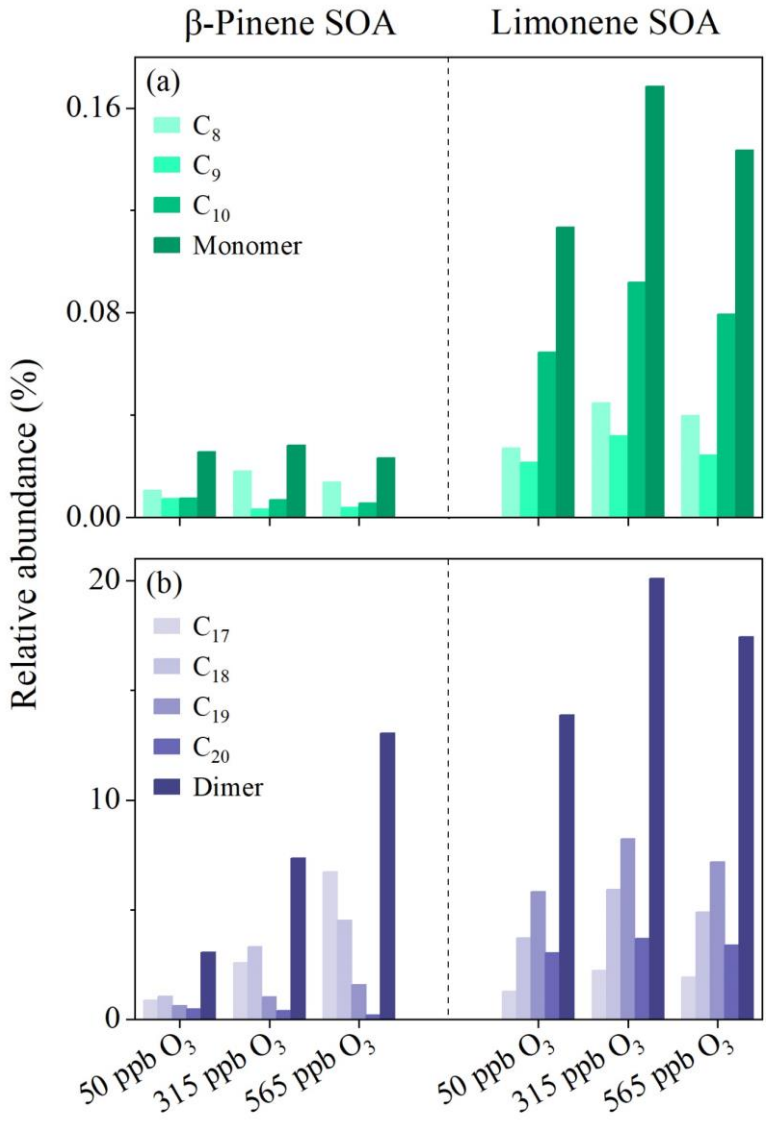


**Figure 6.** The relative abundance of HOMs monomers (a) and dimers (b) identified in β-pinene and limonene SOA as a function of carbon number ($C_n$).

https://doi.org/10.5194/acp-2022-636
Preprint. Discussion started: 13 September 2022


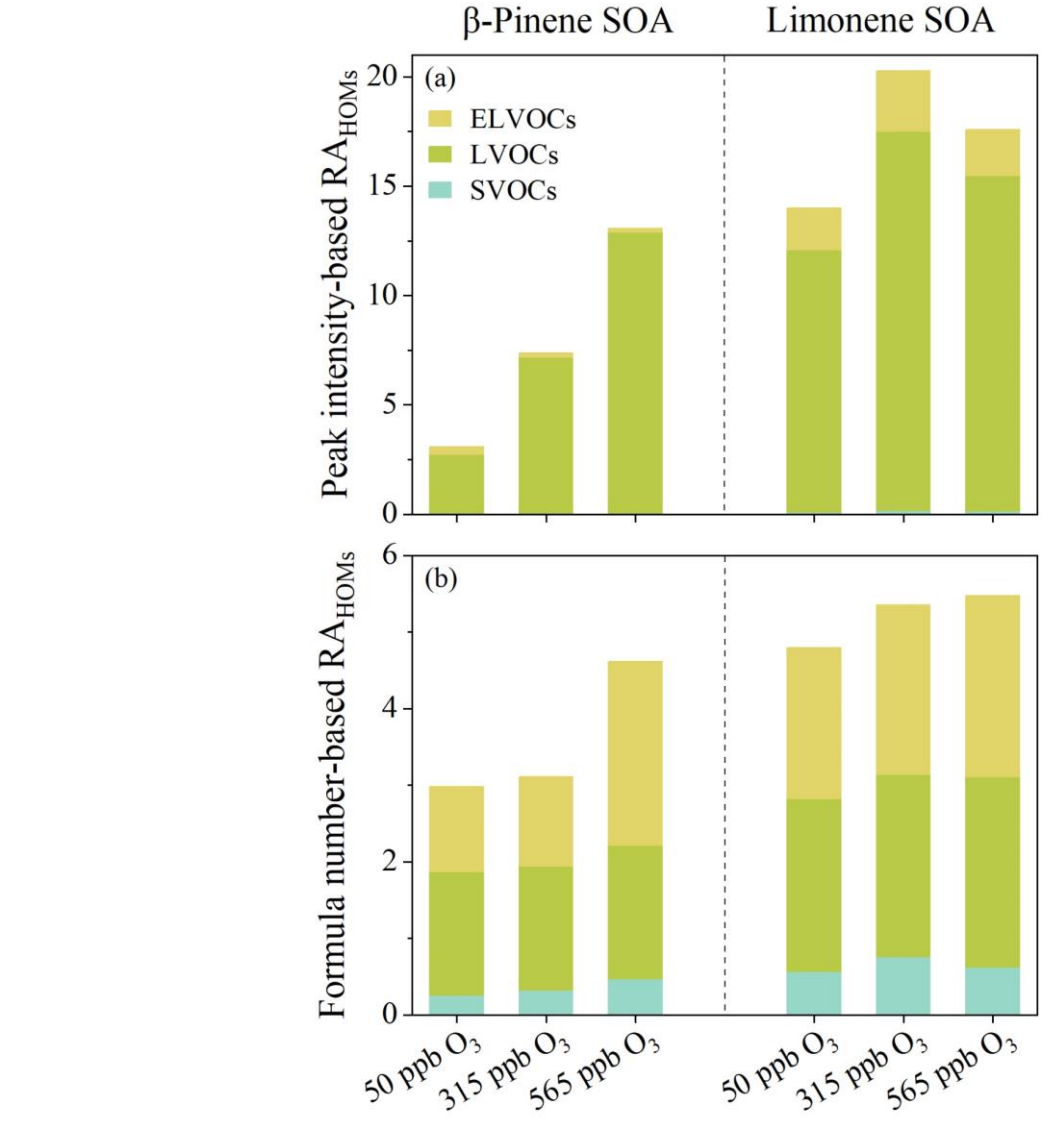


**Figure 7.** The peak intensity- (a) and formula number- (b) based relative abundance of HOMs with different volatilities in SOA particles produced from ozonolysis of β-pinene at and limonene under the three ozone concentrations.

https://doi.org/10.5194/acp-2022-636
Preprint. Discussion started: 13 September 2022


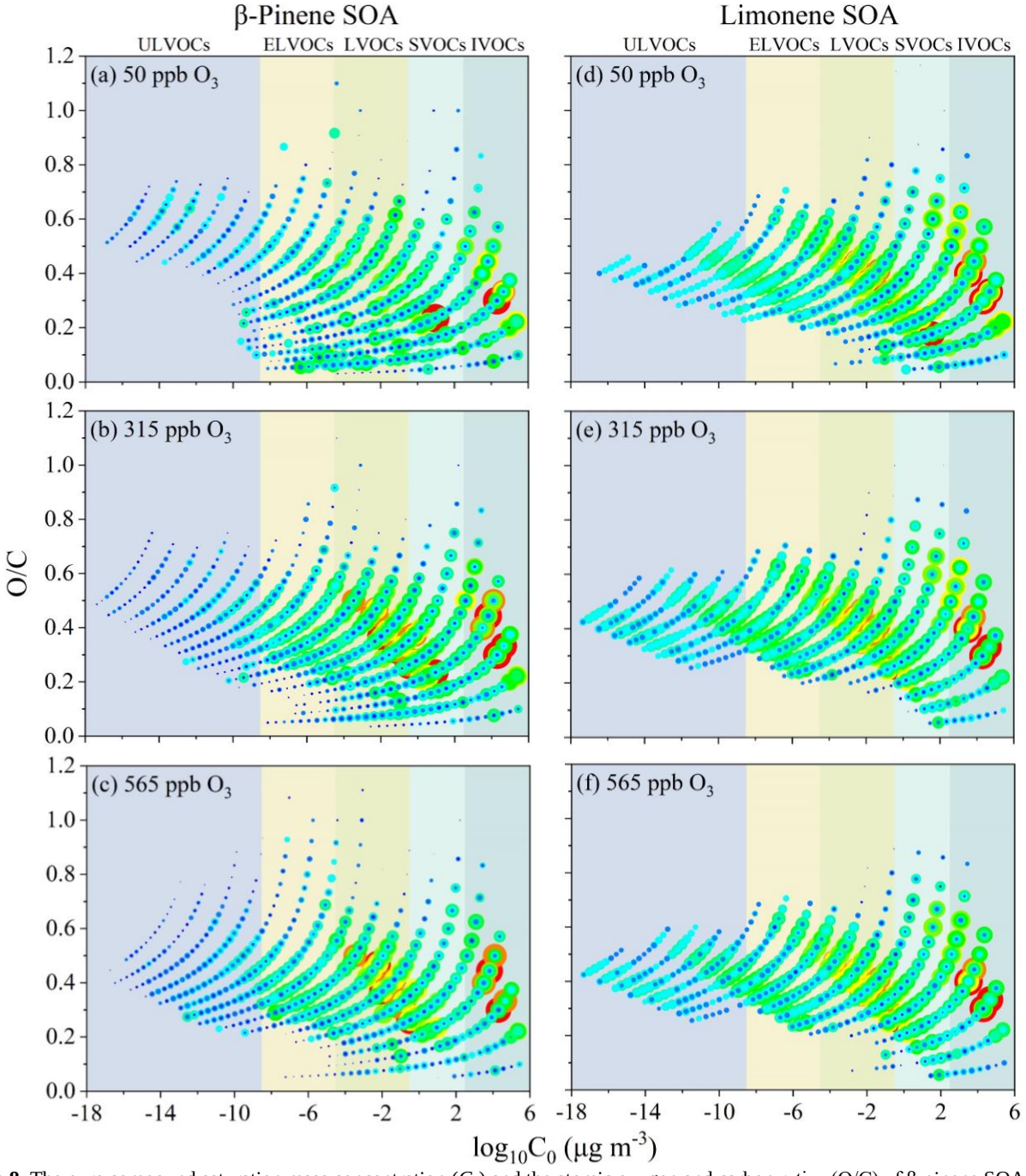


**Figure 8.** The pure compound saturation mass concentration ($C_0$) and the atomic oxygen and carbon ratios (O/C) of β-pinene SOA (a, b, c) and limonene SOA (d, e, f). Markers are color-coded and the dot size is scaled to the logarithm of relative abundance.

https://doi.org/10.5194/acp-2022-636
Preprint. Discussion started: 13 September 2022


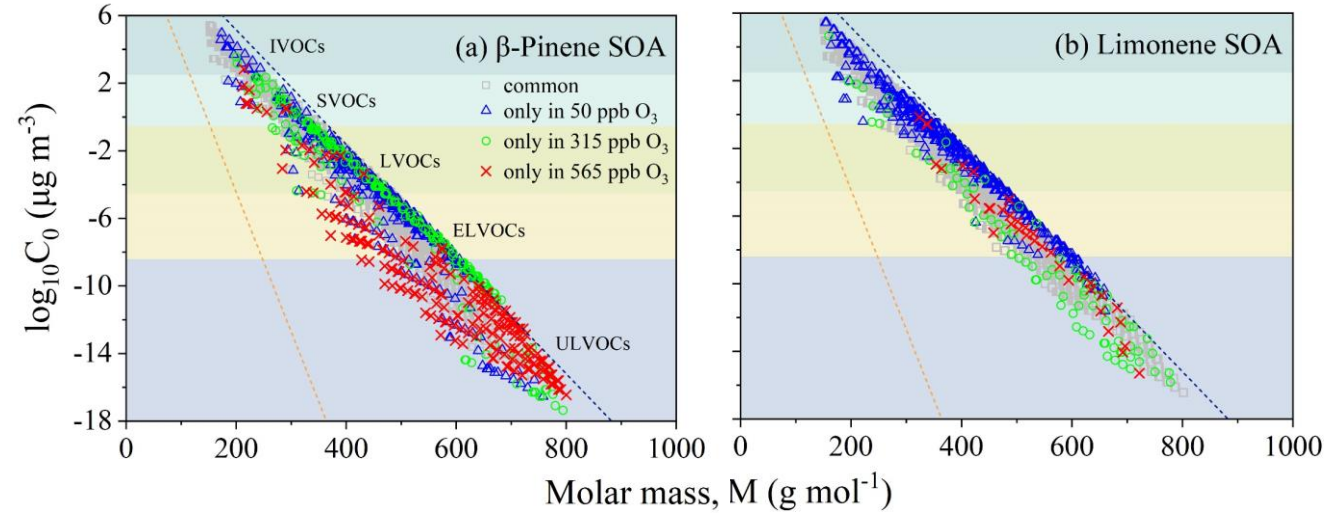


**Figure 9.** Molecular corridors of β-pinene (a) and limonene SOA (b) formed at 50 ppb, 315 ppb and 565 ppb ozone conditions. The gray squares represent the common compounds identified in SOA formed at three different ozone concentrations. The blue triangles, green circles, and red crosses indicate compounds only found in 50, 315, and 565 ppb ozone, respectively. The dotted lines represent linear *n*-alkanes $C_nH_{2n+2}$ (blue with O/C = 0) and sugar alcohols $C_nH_{2n+2}O_n$ (orange with O/C = 1).

https://doi.org/10.5194/acp-2022-636
Preprint. Discussion started: 13 September 2022


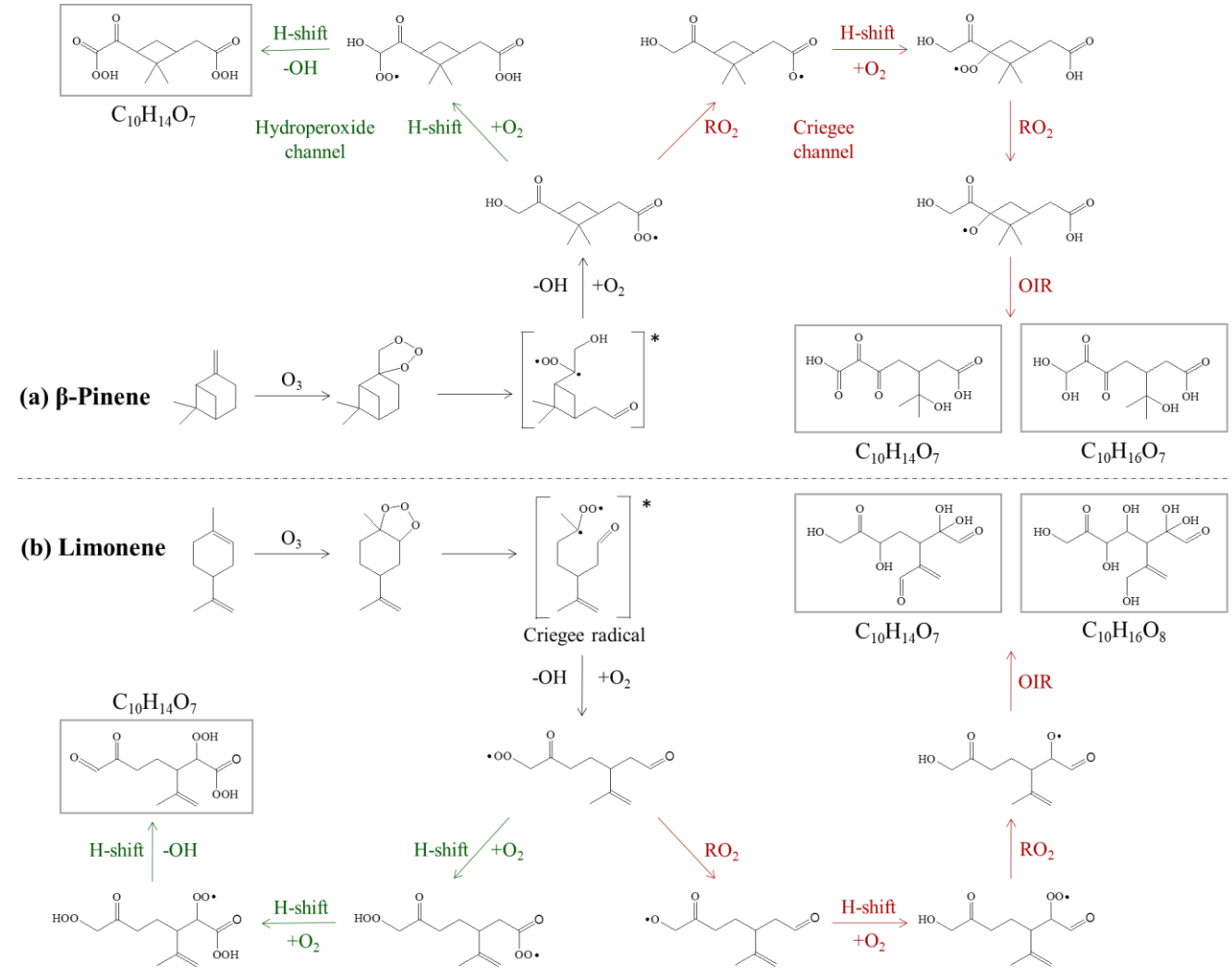


**Figure 10.** Proposed formation mechanism of $C_{10}$ HOMs from the β-pinene and limonene ozonolysis via hydroperoxide channel (green) and oxygen-increasing reactions (OIR) (H-shift → $O_2$ → $RO_2$) of Criegee channel (red) (Tomaz et al., 2021; Shen et al., 2021; Kundu et al., 2012). The organic molecules in the gray rectangle are the hypothesized structures.

https://doi.org/10.5194/acp-2022-636
Preprint. Discussion started: 13 September 2022


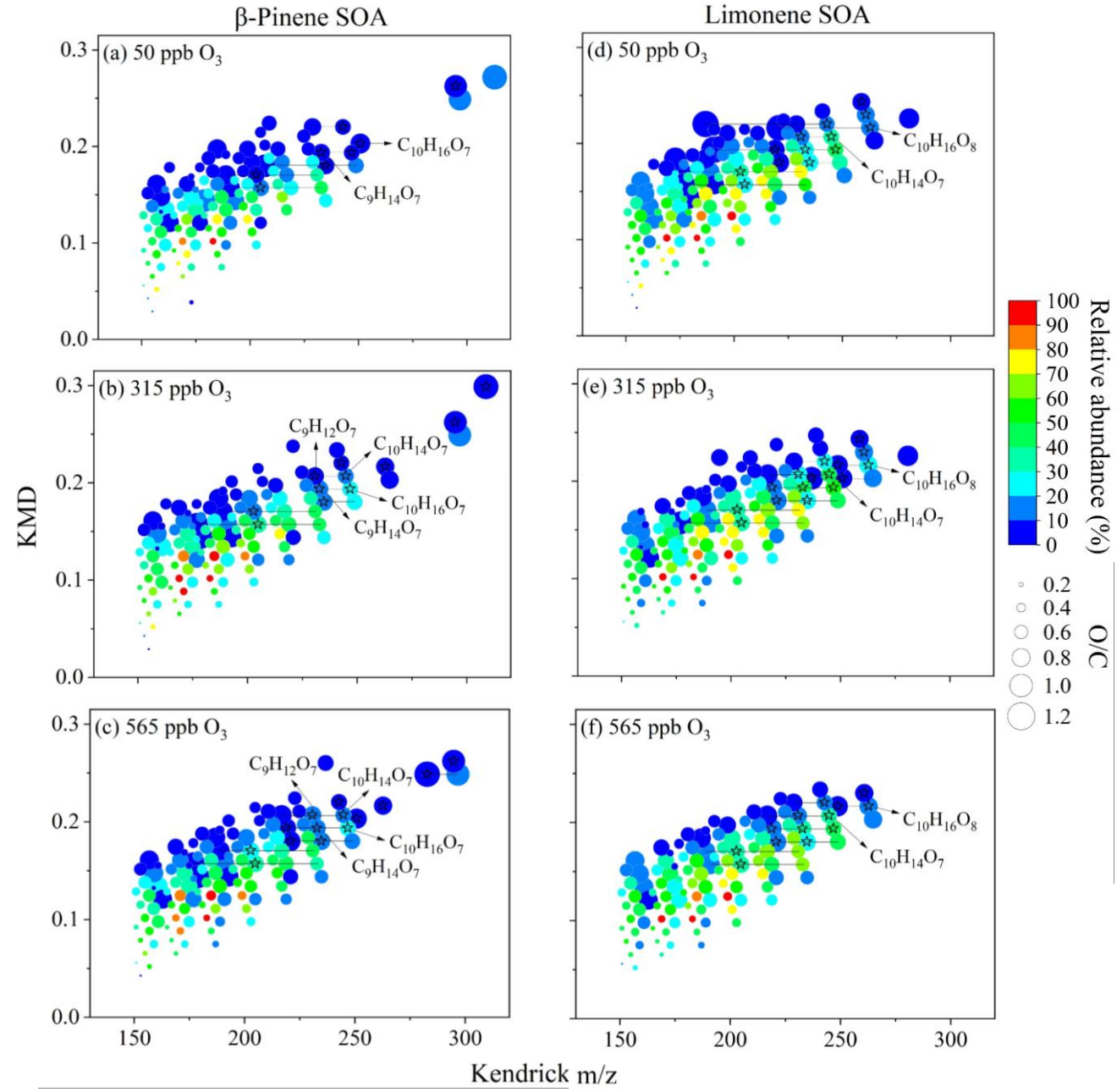


**Figure 11.** Kendrick mass defect of detected organic compounds in β-pinene SOA (a, b, c) and limonene SOA (d, e, f). Different colors represent the logarithm of relative abundance. Different dot sizes denote the atomic ratio of oxygen to carbon (O/C). The black pentagrams delegate HOMs.